Scilight

Sustainable Engineering Novit

https://www.sciltp.com/journals/sen

Review

Recent Progress on Photoelectrochemical Valorizations: A Review of Reactions, Catalyst Design, and Future Prospects

Juntong Jiao [1], Haiqi Wei [1], Qian Lei [2], Jiale Wang [1], Yuru Yang [1], Yuankai Li [2] and Chengkai Xia [1,*]

[1] School of Materials Science and Engineering, Collaborative Innovation Center of Ministry of Education and Shanxi Province for High-performance Al/Mg Alloy Materials, North University of China, Taiyuan 030051, China
[2] School of Chemical Engineering, Sungkyunkwan University (SKKU), 2066 Seobu-ro, Jangan-gu, Suwon 16419, Republic of Korea
* Correspondence: ckxia@nuc.edu.cn

How To Cite: Jiao, J.; Wei, H.; Lei, Q.; et al. Recent Progress on Photoelectrochemical Valorizations: A Review of Reactions, Catalyst Design, and Future Prospects. *Sustainable Engineering Novit* **2026**, *2*(2),5. https://doi.org/10.53941/sen.2026.100010

Received: 27 January 2026
Revised: 24 March 2026
Accepted: 3 April 2026
Published: 24 June 2026

Abstract: Photoelectrochemical (PEC) cells have been considered a promising technology for converting solar energy into chemical energy. However, the solar-to-hydrogen (STH) conversion efficiency and cost-effectiveness of PEC water splitting are significantly limited by the sluggish oxygen evolution reaction (OER) kinetics and the poor economic of the produced oxygen gas, hindering the practical commercialization of PEC energy conversions. In recent years, PEC valorizations including alternative OER and HER reactions have attracted considerable attention. PEC valorizations not only improve STH efficiency but also enhances the overall economic benefits of PEC conversions. Thereby, this review briefly summarizes the basic mechanisms several typical types of PEC value-added reactions, including nitrogen reduction, nitrogen oxide reduction, ammonia oxidation, urea oxidation, and alcohol oxidation reactions. Subsequently, the design and optimization strategies of photoelectrode materials applied to these PEC value-added reactions are specifically analyzed. Finally, the current development, future prospects, and challenges toward commercial-scale applications are discussed.

Keywords: photoelectrochemical; catalyst; nitrogen reduction reaction; alcohols oxidation reaction; value-added production

1. Introduction

The escalating global energy crisis and environmental degradation have emerged as two profoundly interconnected challenges that pose significant threats to sustainable development worldwide. Fossil fuel combustion, which accounts for over 80% of global primary energy consumption, not only depletes non-renewable resources but also severely disrupts natural nitrogen and carbon cycles through excessive emissions of carbon dioxide (CO_2) and nitrogen oxides [1]. The natural nitrogen cycle, mediated by microorganisms such as nitrogen-fixing bacteria and nitrifiers, operates at a relatively slow rate, which is insufficient to meet the exponentially growing agricultural demand for nitrogen-based fertilizers [2]. This imbalance has led to the overreliance on the Haber-Bosch process for ammonia synthesis, which consumes approximately 2% of global energy and contributes about 3% of anthropogenic CO_2 emissions [3]. At the same time, the natural carbon cycle, which was traditionally balanced by photosynthesis and respiration, is now overburdened by anthropogenic carbon dioxide emissions, resulting in a 50% increase in atmospheric carbon dioxide concentration since the Industrial Revolution [4]. These systemic disruptions underscore the urgent need to develop environmentally friendly chemical production technologies and clean energy sources. These technologies can not only reduce pollutant emissions but also transform low-value nitrogen- and carbon-containing feedstocks into high-value chemicals [5].

Photocatalysis, recognized as a promising sustainable technology, has been widely investigated for artificial nitrogen fixation and hydrogen evolution reaction since the landmark discovery of photocatalytic water splitting by Fujishima and Honda in 1972 [6]. However, typical photocatalytic reactions are limited by inherent limitations, such as the rapid recombination of photogenerated electron-hole pairs and insufficient redox potentials for activating inert molecules such as N_2 and CO_2, resulting in unsatisfactory conversion efficiency for the past decades [7]. To address these limitations, photoelectrochemical (PEC) catalysis has been developed as an advanced hybrid platform that synergistically couples photocatalytic processes with electrochemical control through the application of an external bias. This integrated approach enables more efficient and tunable catalytic transformations. The applied potential not only facilitates the spatial separation of photogenerated electrons and holes to suppressing charge recombination, but also allows precise modulation of the catalyst's electronic band structure. Such modulation optimizes the alignment between the catalyst's energy levels and the redox potentials required for activating inert molecules, thereby enhancing both activity and selectivity in target reactions [8–10]. Furthermore, the compatibility of PEC with renewable electricity sources positions it as a key enabling technology for sustainable chemical synthesis, offering a pathway to mitigate anthropogenic emissions while converting low-value feedstocks into value-added products (Figure 1).

For cathode conversions, PEC valorizations have demonstrated considerable potential in two pivotal catalytic upgrading pathways: nitrogen fixation and nitrogen oxide (NO_x) reduction. Conventional N_2 fixation via the Haber-Bosch process requires harsh conditions (300–500°C, 150–300 atm), rendering it highly energy-intensive and environmentally detrimental. In contrast, PEC N_2 fixation proceeds under ambient conditions, utilizing solar energy and water as the proton source. These separated charges drive the multi-electron, proton-coupled reduction of inert N_2 to ammonia or other nitrogenous compounds, typically using water as a sustainable proton source. The overall efficiency is governed by the catalyst's ability to adsorb and activate the N≡N bond, alongside effective interfacial charge transfer kinetics [11]. Similarly, in PEC NO_x reduction, the technology leverages a comparable photoelectrochemical framework to convert various oxidized nitrogen species (e.g., nitrate, nitrite) into value-added products like ammonia [12]. This pathway not only mitigates an environmental pollutant but also recovers nitrogen resources, with performance hinging on the selectivity of the catalyst surface towards desired reduction pathways over competing reactions, such as hydrogen evolution reaction and CO_2 reduction reaction [13].

In addition, PEC valorizations on anode side also play a transformative role in building the organic upgrading technology system, focusing on the conversion of liquid organic chemicals. Its basic purpose is to use photosensitive electrodes to drive organic molecules to be converted into H_2 fuel with high energy density and fine chemicals with high added value. During the reaction, the photoanode provides photogenerated highly oxidizing holes that selectively convert organic molecules into high-value fine chemicals and generate H_2 gas at the cathode, thereby integrating clean energy production and chemical synthesis into a single solar-driven process. The key challenges of PEC organic upgrading studies are controlling the reaction selectivity towards multi-carbon products, which requires precise management of consecutive proton-coupled electron transfer steps and the catalytic promotion of carbon-carbon bond formation. The applied bias in PEC systems is critical for modulating the interfacial potential and stabilizing key reaction intermediates, thereby steering product distribution [14].

Despite the significant potential of PEC catalytic process for nitrogen conversions and organic upgrading, their commercial application is limited by several challenges. First, there is the challenge of simultaneously achieving high efficiency and high product selectivity. This target is hindered by the inherent characteristics of photoanode materials, such as insufficient utilization of the solar spectrum, rapid recombination of photogenerated carriers, and the inherent difficulty in activating stable molecules such as N_2 and CO_2, which lead to competitive reactions [15,16]. Secondly, the long-term stability of photoelectrodes remains a major concern, as the combined effects of light, applied bias, and corrosive electrolytes can induce photo-corrosion or surface reconstruction, resulting in performance degradation over time [17,18]. Finally, a comprehensive mechanistic understanding of the catalytic upgrading processes is still lacking. The reaction kinetics at the solid-liquid interface and the reaction pathways controlling the formation of high value-added multi-carbon or multi-nitrogen products have not yet been explored, and these theoretical gaps hinder the rational design of optimized systems [19].

This review provides an overview of the fundamental mechanisms of PEC valorizations and introduces a series of catalytic processes aimed at producing value-added chemicals, replacing the sluggish oxygen evolution reaction (OER) and hydrogen evolution reaction (HER). The relevant strategies and mechanisms are also emphasized in depth. In this review, we firstly summarized the basic mechanisms of PEC reduction of nitrogen compounds and oxidation of organic compounds, and explain the charge transport and transfer behavior at photoelectrode/electrolyte interfaces. Second, for different anodic reactions, we propose strategies to enhance direct charge transfer on the photoanode surface to control the conversion pathway and improve conversion efficiency, including surface composition modulation, vacancy engineering, heterostructure construction, metal

loading, and co-catalyst coating. Third, we systematically summarize and compare the kinetic mechanisms of different modification measures in regulating photoanode reactions. Finally, we discuss current challenges and future development directions. We hope this review will provide valuable guidance for researchers dedicated to the efficient design of photoelectrodes and the value-added conversion of small molecules [20].

In PEC systems, the operational definition of 'value-added conversion' refers to the economic gain of the photochemical process, quantified by measuring the formation rate and Faradaic efficiency of the target product, with the market price or energy density of the product relative to that of the reactants serving as the core indicator. Additionally, the operational definition of "selective oxidation" refers to the regulation of the catalyst and the reaction microenvironment to ensure that hole-mediated oxidation reactions proceed preferentially along the target pathway, with the percentage of the target product relative to the total products serving as the metric for evaluating the control of the reaction pathway.

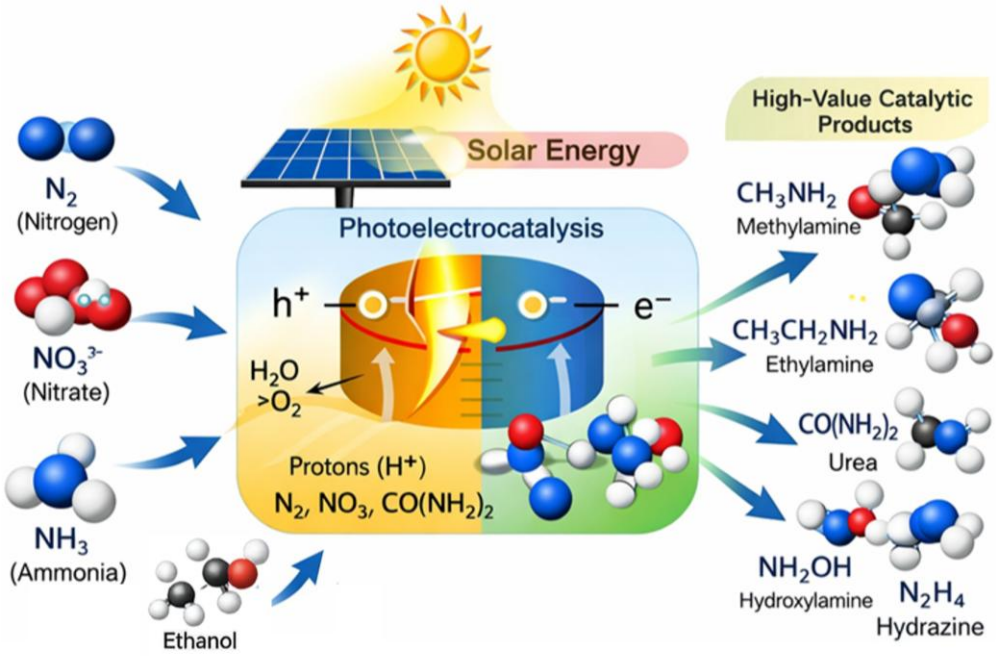

Figure 1. Schematic of PEC valorizations.

2. Fundamentals of PEC Cells for Valorizations

2.1. Fundamentals of Photoanode Reactions

PEC catalysis represents a synergistic process that incorporated the light-harvesting capability of photocatalysis with the bias-control of electrocatalysis, enabling the direct conversion of solar energy into chemical energy for driving catalytic upgrading reactions. A typical PEC water splitting cell uses two electrodes to generate oxygen and hydrogen respectively. The anode undergoes water oxidation through a four-proton coupled electron transfer process, while the cathode releases hydrogen through a two-electron reduction reaction. The basic principle of a PEC upgrading catalysis, especially at the photoanode, follows a sequential and interconnected multi-step process, which determines its overall efficiency [21]. The basic mechanism of photoanode reactions relies on three interconnected processes: light absorption by the photoanode semiconductors, separation and transfer of photogenerated charge carriers, and surface redox reactions with target molecules [22].

The initial step involves photon absorption by the semiconductor photoanode. Upon irradiation with light of energy equal to or greater than its bandgap energy (E_g), electrons in the valence band (VB) are excited to the conduction band (CB), generating electron-hole (e^-/h^+) pairs. The spectral range of absorbed light is intrinsically determined by E_g, dictating the portion of the solar spectrum that can be utilized [23]. Metal oxides with n-type semiconductor properties are widely used as photoanode catalysts due to their superior chemical stability, suitable band edge positions, tunable band gaps, and low cost, including zinc oxide (ZnO), titanium dioxide (TiO_2), tungsten oxide (WO_3), bismuth oxide ($BiVO_4$), hematite (α-Fe_2O_3), etc.

The effective spatial separation and transport of these photogenerated charge carriers are critical. A key challenge is the rapid recombination of e^-/h^+ pairs, which diminishes the population of available charges for

surface reactions [24]. The application of an external anodic bias plays a pivotal role in mitigating this loss. It establishes an electric field within the semiconductor that drives the photogenerated holes toward the electrode/electrolyte interface while directing electrons through the external circuit toward the cathode, thereby achieving vectorial charge separation [8]. This process is further enhanced through intrinsic material engineering strategies designed to create built-in electric fields or favorable energy alignments that facilitate the directional flow of holes.

The final and functionally decisive step is the surface oxidation reaction. The photogenerated holes that successfully migrate to the photoanode surface participate in oxidative half-reactions with adsorbed species or solvent molecules. The thermodynamic feasibility of these oxidation reactions is contingent upon the energy position of the valence band, which must provide sufficient oxidative potential relative to the redox couple of interest. The kinetics and selectivity of these multi-hole transfer processes, often involving the formation of reactive oxygen species or the direct oxidation of substrates, are central to driving the targeted transformations within artificial cycles. Thus, the overall efficiency of organic conversion is determined by the light collection, charge transport, and transfer efficiency of the semiconductor photoelectrode.

2.2. Evaluation of a Photoelectrode and PEC Conversion Efficiency

2.2.1. Faradaic Efficiency (FE)

FE measures the percentage of electrons used for the target product, relative to the total electrons passed (via Faradaic current). It is the most widely used metric for evaluating reaction selectivity [25,26]. FE requires two key inputs: total Faradaic charge $\left(Q_{\text{Faradaic, total}}\right)$from current measurements, and moles of target product $\left(n_{\text{product}}\right)$ from analytical techniques [25]. For a target product formed via n_e electrons per mole, FE is calculated as:

$$\text{FE}(\%) = \frac{Q_{\text{product}}}{Q_{\text{Faradaic, total}}} \times 100 = \frac{n_{\text{product}} \times n_e \times F}{Q_{\text{Faradaic, total}}} \times 100$$

where: Q_{product} = charge consumed for target product (C),

n_e = number of electrons transferred per mole of product (dimensionless),

F = Faraday's constant (96,485•C/mol e^-),

$Q_{\text{Faradaic, total}}$ = total Faradaic charge (C) from $\int I_{\text{Faradaic}} dt$.

To ensure accuracy, the sum of FEs for all detected products (target + side products) should approach 100%. For example, in CO_2 reduction, $\text{FE}_{\text{CO}} + \text{FE}_{\text{CH}_4} + \text{FE}_{\text{H}_2} \approx 100\%$, confirming no unaccounted electron loss.

2.2.2. Product Yield

Yield quantifies the amount of target product generated, critical for assessing PEC system scalability. It is expressed in two common forms: molar yield (reactant conversion) and mass/time yield (production rate) [27]. Molar yield (Y_{molar}) measures the ratio of moles of target product to moles of reactant consumed, reflecting reactant conversion efficiency:

$$Y_{\text{molar}}(\%) = \frac{n_{\text{product}}}{n_{\text{reactant, consumed}}} \times 100$$

$n_{\text{reactant, consumed}}$ is calculated as the initial moles of reactant minus residual moles (measured via analytical techniques, e.g., ion chromatography for nitrate). Mass/time yield $(Y_{\text{mass-time}})$ quantifies product generation rate per unit catalyst mass, used to compare catalyst activity across studies. The formula is:

$$Y_{\text{mass-time}} = \frac{m_{\text{product}}}{m_{\text{catalyst}} \times t}$$

where: $m_{\text{product}} = massoftargetproduct(mgor\mu g)$

$m_{\text{catalyst}} = massofactivecatalyst(g)$,

$t = reactiontime(h)$.

2.3. Requirements for Photoanode Materials

Photoanodes in photoelectrochemical cells must effectively execute the three fundamental processes of light absorption, charge separation/transport, and surface oxidation. Their theoretical performance, such as solar-to-hydrogen (STH) efficiency and photocurrent density, is primarily governed by the material's band structure. While a narrower bandgap is generally desirable for enhanced light absorption, and the valence band maximum must be

positioned to thermodynamically enable water oxidation, an excessively small bandgap can induce rapid charge recombination and insufficient photovoltage, thereby limiting practical performance.

The experimentally achieved efficiencies of common n-type semiconductor photoanodes remain significantly below their theoretical limits, mainly due to two interrelated challenges: inefficient charge carrier separation and transport caused by bulk defects or interfacial energy barriers, and severe charge recombination that slows surface reaction kinetics. To address these issues, diverse engineering strategies have been developed. These include morphology and crystal facet engineering to optimize light absorption and expose active sites, modulation of doping and defect concentrations to improve bulk conductivity, and the application of co-catalysts or surface functionalization layers to accelerate interfacial charge transfer and catalytic kinetics.

For future implementation in commercial-scale, photoanode design must also meet criteria for scalability and integration into unbiased devices. Interface engineering is particularly critical, as optimizing the space charge layer and mitigating surface states can reduce the overpotential for water oxidation. This facilitates a cathodic shift in the photocurrent onset potential, which is essential for constructing efficient, standalone PEC systems. Among various approaches, constructing heterojunctions has emerged as a predominant strategy, as it can simultaneously modulate the band structure and passivate surface defects. Consequently, developing precise and broadly applicable methods for building such heterostructures remains a central research focus.

2.4. Mechanism of Photocathode Materials

"In PEC reactions, the fundamental mechanism of photocathodes involves the core process whereby semiconductor materials convert light energy into chemical energy under illumination to drive reduction reactions: when the energy of incident photons is greater than or equal to the bandgap of the photocathode material, electrons in the valence band are excited and transition to the conduction band, forming photo-generated electron-hole pairs; Subsequently, driven by the built-in electric field, the photo-generated electrons migrate directionally towards the electrode surface, whilst the holes migrate towards the bulk or the counter electrode, thereby effectively suppressing carrier recombination. Finally, the high-energy electrons that have migrated to the surface participate in interfacial charge transfer, undergoing reduction reactions with electron acceptors in the solution to generate target products, thereby completing the conversion of solar energy into chemical bond energy.

3. Photocathode Conversions

PEC systems, the photocathode traditionally facilitates reduction reactions, with the HER representing the most common and energetically favorable pathway. To pursue higher-value chemical products, research has increasingly shifted toward alternative cathodic reductions, notably the nitrogen reduction reaction (NRR) and the nitrate reduction reaction (NORR). This transition responds to the limitations of conventional industrial nitrogen fixation, especially the Haber–Bosch process, which operates under harsh conditions of high temperature and pressure, accounts for 1–2% of global energy consumption, and emits roughly 1.8 tons of CO_2 per ton of ammonia produced [28–30]. Its inefficiency within the natural nitrogen cycle further motivates the development of greener and less energy-intensive alternatives.

Thereby, PEC reduction reactions on photocathodes present distinct advantages over thermal catalytic routes. They proceed under ambient temperature and pressure, can be directly integrated with renewable energy sources such as solar irradiation to lower carbon emissions, and allow precise steering of reaction pathways through modulation of light/electrical parameters and catalyst design. Such control enhances selectivity toward valuable products like ammonia while suppressing competing HER [31]. Consequently, PEC systems not only reduce the complexity and cost of reactor engineering but also mitigate issues such as high-temperature catalyst deactivation, aligning closely with the "dual-carbon" objectives and the principles of green chemistry [32].

3.1. Nitrogen Reduction Reaction

NRR refers to the catalytic conversion of stable atmospheric dinitrogen (N_2) into nitrogen-containing compounds under specific conditions, with the reduction to ammonia (NH_3) representing its core objective. N_2 is one of the most stable diatomic molecules in nature which possesses a high bond dissociation energy. Such a high bond dissociation energy stems from the symmetric electronic structure of the N_2 molecule and its lack of a permanent dipole moment, which hinder effective adsorption onto catalyst surfaces [33,34]. Furthermore, cleaving the N≡N bond requires overcoming a significant energy barrier, rendering conventional catalysts largely ineffective under mild conditions [35].

The main challenge in NRR is its low selectivity. During the reduction process, protons from the electrolyte readily combine with electrons to undergo the competing HER. The standard potentials for HER and NRR are

relatively close, which typically results in poor Faradaic efficiency for NH_3 production and makes highly selective synthesis challenging to achieve [36].

Another key difficulty involves the regulation of reaction intermediates. NRR is a complex multi-electron transfer process that generates various intermediates such as $*N_2$, *NNH, and $*NH_2$. The stability and subsequent conversion pathways of these species directly govern product selectivity. Inadequate control over these intermediates can easily lead to the formation of by-products like hydrazine (N_2H_4) or nitrite (NO_2^-), thereby further diminishing the yield of the desired product NH_3 [37].

The reaction equation is as follows:

$$N_2 + 6H^+ + 6e^- \rightarrow 2NH_3$$

In addition to aqueous inorganic electrolytes, non-aqueous systems with added proton sources are widely employed in PEC NRR. These organic electrolytes enhance N_2 solubility, suppress the competing hydrogen evolution reaction by limiting proton availability, and enable novel reaction pathways such as lithium-mediated nitrogen reduction, which has achieved high Faradaic efficiency. The choice of electrolyte fundamentally influences the reaction mechanism, intermediate stabilization, and overall performance [38].

3.1.1. Bulk Optimization

Bulk optimization refers to the targeted alteration of the core composition and intrinsic structure of a catalyst to modulate the inherent thermodynamic activity of the photoelectrode. This strategy goes beyond surface-level adjustments, focusing on the bulk properties of the material—including atomic arrangement, electronic states, crystal order, and elemental distribution—to fundamentally alter catalytic behavior [39–41]. Typical approaches include tuning the type and stoichiometry of active metals, constructing alloyed or heterostructured phases, engineering crystallographic defects, and fabricating hierarchically porous or layered architectures [42–44]. By directly modulating these inherent properties, researchers aim to overcome key bottlenecks in NRR catalysts: not only by tailoring the electronic structure to weaken the N≡N bond and promote N_2 adsorption and activation, but also by enhancing selectivity toward ammonia through improved hydrophilicity, charge transport, or active-site specificity, thereby suppressing the competing hydrogen evolution reaction. Moreover, such bulk-level modifications frequently contribute to improved electrochemical and structural stability under operating conditions [45].

These mechanisms are well reflected in the development of metal-free catalysts for PEC NRR. For example, Liu and colleagues used ultrathin black phosphorus (BP) nanosheets prepared by electrochemical exfoliation as a metal-free two-dimensional catalyst [46]. As is shown in Figure 2a, direct band gap and high carrier mobility of BP facilitated the efficient separation of photogenerated charges, while its inherent weak hydrogen adsorption significantly suppressed the HER. Furthermore, the applied external bias promoted the extraction of photogenerated holes, mitigated oxidative degradation, and produced a synergistic effect of photoexcitation-enhanced electrocatalysis and bias-enhanced photocatalysis. (Figure 2b) This integrated bulk and interfacial design overcomes the typical activity and stability limitations of metal-free catalysts, achieving an NH_3 generation rate of 102.4 μg h^{-1} mg cat^{-1} and a FE of 23.3% at −0.4 V vs. RHE without the need for sacrificial agents. (Figure 2c)

Similarly, the innovative combination of plasmonic elements with bulk catalytic materials demonstrates how structural and electronic engineering can enhance N_2 activation. Zabelina's team designed a hybrid system that couples a gold grating with TiB_2 modified with gold nanoparticles [47]. As is demonstrated in Figure 2d, the coupling between localized surface plasmons and surface plasmon polaritons concentrates light energy into the TiB_2 interlayer, reaching the sub-diffraction scale, while an ionic liquid electrolyte further suppresses the HER. The resulting strong localized electric field enhances the adsorption of N_2 on the Ti active sites and reduces the dissociation energy of key intermediates. This method effectively overcomes the common problems in traditional TiB_2 catalysts, such as insufficient exposure of active sites and difficulty in N≡N bond activation. (Figure 2f) Under simulated solar irradiation at −0.2 V vs. RHE, the system achieved an NH_3 yield of 535.2 μg h^{-1} $mgcat^{-1}$ with a Faraday efficiency of 31.7% when using pure nitrogen as the nitrogen source. Even when using air as the nitrogen source, the system maintained a high yield of 491.3 μg h^{-1} $mgcat^{-1}$, indicating that utilizing abundant raw materials and driving ammonia synthesis through renewable energy is a feasible approach.

Future research should focus on further optimizing material structures to better match their inherent properties with catalytic requirements; promoting integrated innovation of material types such as metal-free compounds and plasma systems; and advancing scalable device configurations to achieve practical photoelectrochemical ammonia production. These efforts are crucial for advancing sustainable, low-energy nitrogen fixation technologies.

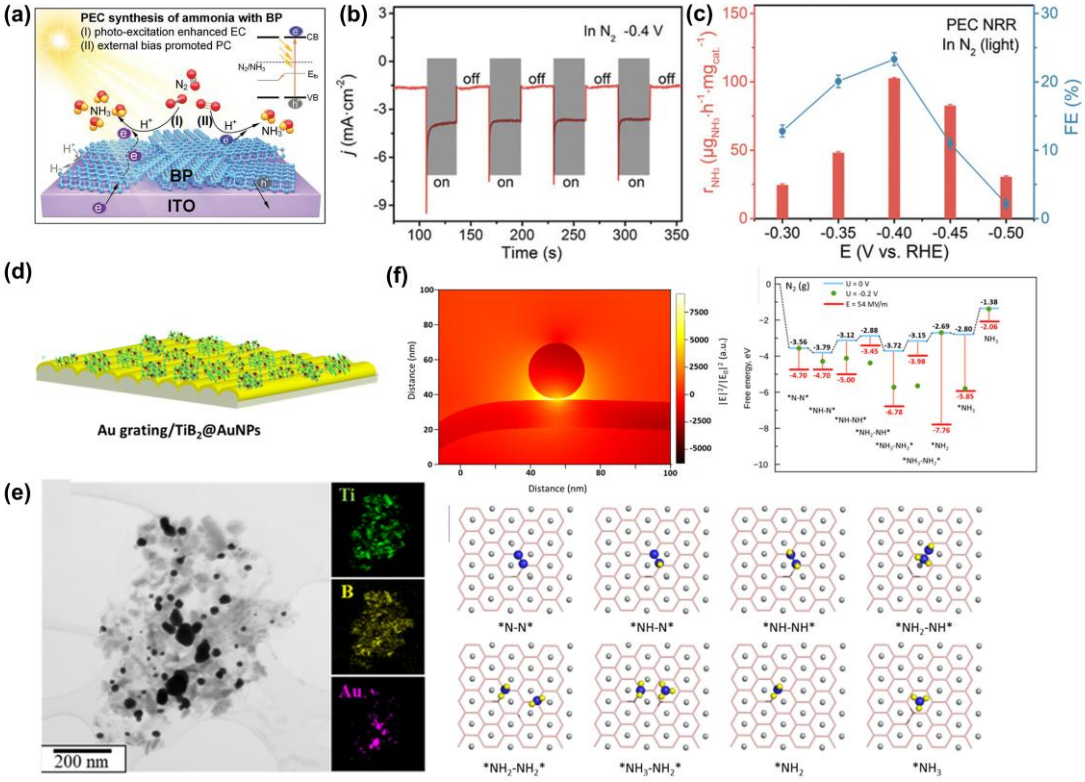

Figure 2. (**a**) PEC NRR enhancement mechanisms of BP under light illustration. (**b**) Light dependent current–time curves of the BP electrode. (**c**) PEC ammonia yield rates and Faradaic efficiency [46]. Copyright 2020, Wiley. (**d**) Schematic concept of the Au grating/TiB_2@AuNP. (**e**) EM image of the TiB_2@AuNP flake and corresponding EDX mapping of Ti, B, and Au. (**f**) FDTD-calculated distribution of the plasmon-related volumetric energy density under the illumination of the coupled AuNP–Au grating system with TiB_2 spacer and DFT stimulations [47]. Copyright 2023, American Chemical Society.

3.1.2. Defect Engineering

Defect engineering refers to the technology of constructing or controlling defect structures such as vacancies, dislocations, and edge sites in catalyst materials through controllable means [48]. Its mechanism of action is to enhance the adsorption and activation of N_2 through defects, optimize carrier separation efficiency, and control the surface electronic states of the material to suppress the competitive HER, thereby improving the ammonia yield and Faraday efficiency of NRR [49].

This strategy has been effectively implemented in recent studies where defect engineering served as a central approach to address key limitations of conventional NRR systems. For example, work led by Li employed a nitrogen-vacancy-modified g-C_3N_5/BiOBr p–n heterojunction [50]. As is shown in Figure 3a, nitrogen vacancies function as electron reservoirs that capture photogenerated electrons from the conduction band of g-C_3N_5 and release them in a controlled manner for N_2 activation. These vacancies also narrow the bandgap of g- C_3N_5, extending its visible-light absorption range. Coupled with the built-in electric field of the heterojunction, they establish a "dual-electron transfer pathway" that significantly suppresses charge recombination and enhances N_2 adsorption—effectively overcoming the low charge-separation efficiency and weak N_2 activation typical of single-semiconductor catalysts. At an applied potential of −0.2 V vs. RHE, this design achieved an NH_3 production rate of 29.4 μg h^{-1} mg^{-1} with a Faradaic efficiency of 11%, without generating detectable hydrazine by-products. (Figure 3b)

In a complementary study demonstrated in Figure 3c, the group led by Ma developed an oxygen-vacancy-modulated V_O-SnO_2/TiO_2 composite photoanode [51]. Oxygen vacancies were introduced into SnO_2 quantum dots via high-temperature annealing under an inert atmosphere. These vacancies create quasi-continuous defect energy levels that narrow the SnO_2 bandgap and serve as electron-trapping sites, facilitating the transfer of photogenerated electrons from the TiO_2 conduction band to SnO_2 and thus reducing carrier recombination. Additionally, the vacancies strengthen N_2 adsorption and lower the activation energy barrier for N≡N bond cleavage. (Figure 3d)

This defect-engineered system addresses the common drawbacks of TiO_2-based catalysts—limited visible-light utilization and poor NRR selectivity—yielding an NH_3 formation rate of 19.41 μg h^{-1} mg^{-1} at −0.2 V vs. RHE with a Faradaic efficiency of 59.6%, along with notable operational stability. (Figure 3e)

Collectively, well-designed defect engineering can enhance NRR performance through vacancy-mediated charge modulation and band structure manipulation, thus providing a feasible design strategy for efficient, stable, and highly selective nitrification NRR photoelectrochemical catalysts.

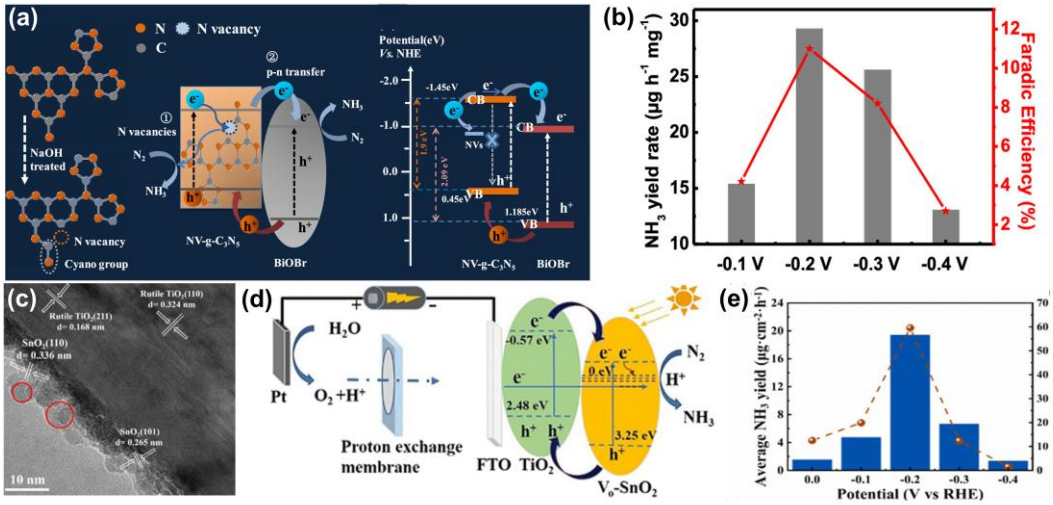

Figure 3. (**a**) Representation of the Double Charge Transfer and NRR Mechanism and the Energy Band Structure of NV-g-C_3N_5/BiOBr. (**b**) NH_3 yield and FE of Ru decorated Cu_2O with different bias [50]. Copyright 2020, American Chemical Society. (**c**) High-angle annular dark field scanning transmission electron microscopy (HAADF–STEM) image. (**d**) Schematic mechanism of the PEC nitrogen fixation reaction in V_o-SnO_2/TiO_2. (**e**) NH_3 yield and faradaic efficiency of V_o-SnO_2-16/TiO_2 at different potentials [51]. Copyright 2024, Royal Society of Chemistry.

3.1.3. p-n Junction Construction

By constructing a p-n junction, a built-in electric field can be generated as electrons and holes diffuse across the interface, utilizing the difference in carrier concentration between p-type and n-type semiconductors, thereby establishing a directional path for charge transport [52]. This electric field promotes efficient separation of photogenerated carriers, reduces recombination losses, and provides sufficient active charge for surface reactions. In addition, by enabling the band structure to match the thermodynamic requirements of NRR, the junction helps to suppress competitive HER. Interfacial coupling can also enhance the chemical stability of the components, thereby extending the catalyst lifetime and supporting the high efficiency of the NRR system [53].

These strategies have been clearly reflected in recent heterojunction-based NRR systems. Gao et al. constructed a double heterojunction structure containing a CoFe-LDH/$BiVO_4$ p-n junction photoanode and a Ru single-atom modified Cu_2O cathode [54]. CoFe-LDH is grown on $BiVO_4$ by hydrothermal method to form a p-n heterojunction, whose built-in electric field accelerates the separation of photogenerated electron-hole pairs. (Figure 4a) Simultaneously, the synergistic interaction of Co and Fe active sites provides additional photogenerated electrons for NRR. On the cathode side, Ru single atoms are anchored to Cu_2O via photo-deposition, forming a metal-single-atom/semiconductor interface. The interaction between the d orbitals of Ru and the N_2 π* orbitals decrease the energy barrier for the formation of the *NNH intermediate, while the adsorption tendency of Cu_2O for nitrate further suppresses HER. (Figure 4b) This dual heterojunction design effectively solves the problems of low charge transport efficiency and insufficient active sites commonly found in single-electrode systems, achieving an NH_3 yield of 230 μmol h^{-1} $gcat^{-1}$ at 0.9 V vs. RHE, with a Faraday efficiency of 14.9%. (Figure 4c)

Huang's team employed a different approach, developing an integrated "artificial blade" system based on an InGaP/GaAs/Ge triple-junction heterostructure coupled to a Ti/Au interface layer [55]. As is shown in Figure 4d and 4e, the triple junction was fabricated by molecular-beam epitaxy, stacking InGaP, GaAs, and Ge to achieve broad-spectrum light absorption and enhanced photovoltage. A sputtered Ti/Au bilayer was subsequently deposited on the InGaP surface, where the Ti layer improved interfacial adhesion and electron transfer between

Au and the semiconductor, while the Au layer provided catalytic sites for NRR and steered the N_2 hydrogenation pathway. (Figure 4f) This multi-junction design overcomes the limited photovoltage of single semiconductors, which typically require external bias. The synergistic interfacial effects yielded a Faradaic efficiency of 28.9% and a STA conversion efficiency of 1.11% under 0.2 sun illumination, with an NH_3 production rate of 8.5 μg cm^{-2} h^{-1} at 1.5 sun illumination. (Figure 4g) This approach illustrates a viable pathway toward the industrialization of solar-driven ammonia synthesis through precise heterojunction engineering.

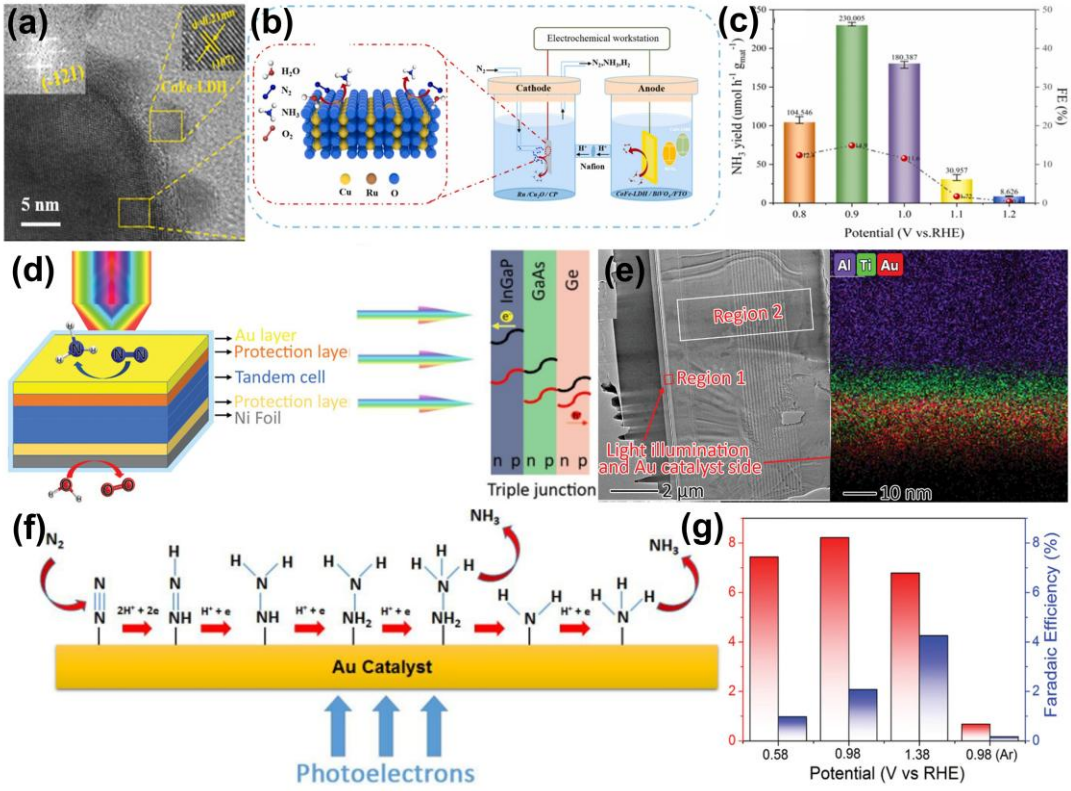

Figure 4. (**a**) HR-TEM images of CoFe-LDH/$BiVO_4$. (**b**) Schematic illustration of the PEC NRR mechanism. (**c**) NH_3 yield and FE of Ru decorated Cu_2O with different bias [54]. Copyright 2025, Elsevier. (**d**) Schematic illustration of the artificial leaf for nitrogen reduction using a 3J InGaP/GaAs/Ge cell with Au catalyst for the nitrogen reduction reaction (NRR) and Ni foil. (**e**) High-angle annular dark field scanning transmission electron microscopy image. (**f**) Schematic illustration of the nitrogen reduction following the alternating pathway on the Au catalyst surface with the assistance of photoelectrons. (**g**) Corresponding ammonia production rate (**left column**) and Faradaic efficiency (**right column**) of the Au/Ti/3J InGaP/GaAs/Ge cell with various bias potential [55]. Copyright 2023, Wiley.

3.1.4. Co-Catalyst Modification

Co-catalyst modification represents a prevalent kinetic optimization strategy in PEC catalysis, wherein suitable co-catalysts are loaded onto light-absorbing semiconductors to promote or accelerate the photocatalytic process [56]. In such systems, co-catalysts primarily function as active reaction sites, catalyzing specific surface redox reactions [57]. Moreover, the interface or junction formed between the co-catalyst and the semiconductor facilitates charge separation and transport, thereby enhancing overall photoconversion efficiency [58]. Typical co-catalysts are categorized based on their composition and structure, including noble-metal-based nanoparticles, transition-metal oxides, layered double hydroxides (LDHs) [59], and emerging single-atom catalysts (SACs) [60]. Each class contributes distinct electronic, geometric, or catalytic properties that can be tailored to improve activity, selectivity, and stability in photoelectrochemical reactions.

SACs are a typical class of cocatalysts, in which isolated metal or non-metal atoms are uniformly dispersed and anchored on the surface or within the lattice of a catalyst support through coordination, adsorption, or similar methods [61]. This strategy maximizes atom utilization and allows for precise tuning of the local electronic structure around the single-atom sites. In PEC-NRR, SACs enhance the interaction between the photoelectrode and N_2, lower the activation barrier for N≡N bond breaking, and suppress the competitive HER, thereby increasing

ammonia yield and Faradaic efficiency [62]. Furthermore, the synergistic effect between the single atom and the support often contributes to improved overall catalytic stability [63,64].

The integration of SACs into dual-electrode PEC configurations effectively demonstrates these advantages. A carefully designed SACs can effectively address specific challenges in PEC NRR, enabling the tandem catalytic process. As is shown in Figure 5a, He's laboratory has developed a layered Au/porous carbon nitride (PCN) catalyst with Au SACs that achieves spatial decoupling between light absorption and catalytic reaction [65]. The combination of PCN and Au nanoparticles enhances N_2 adsorption and lowers the activation barrier of the N≡N bond. (Figure 5b) Therefore, this system achieves an NH_3 production rate of 13.8 μg h^{-1} mg^{-1} and a Faradaic efficiency of 61.8% at a low bias of −0.10 V vs. RHE, providing an effective approach to balancing light capture and catalytic activity. (Figure 5c)

As is shown in Figure 5d, in another strategy, a ternary heterostructure of Mo_2C/GaN/InGaN nanowires was constructed to improve charge transfer and stability in acidic media [66]. A GaN buffer layer forms a type-I heterojunction with InGaN and establishes a low-offset conductive interface with Mo_2C, enabling efficient electron transfer from the photo-accepter to the catalytic sites. (Figure 5e) This design mitigates the poor stability and limited charge transport of bare InGaN nanowires, yielding an NH_3 production rate of 7.93 μg h^{-1} mg^{-1} with a Faradaic efficiency of 15.39% at −0.2 V vs. RHE. (Figure 5f)

Transition metal oxides are also widely used as PEC co-catalyst. For example, in Figure 5g, Ti-doped WO_3/$SrWO_4$ hybrid photocathode was designed to enhance charge separation and reaction selectivity [67]. Doping with Ti modifies the interfacial electronic structure between WO_3 and $SrWO_4$, which reduces carrier recombination and favors NRR over HER. (Figure 5h) The Ti-doped WO_3 co-catalyst delivered an NH_3 yield of 11.17 μg h^{-1} mg^{-1} with a Faradaic efficiency of 13.42% at −0.5 V vs. RHE, overcoming the limitations of the individual oxide catalysts. (Figure 5i)

These works demonstrate rationally designed co-catalysts can synergistically improve light absorption, charge transport, and catalytic activity in PEC-NRR systems. Future efforts might focus on refining interfacial compatibility, precisely aligning band structures across multiple components, and developing robust multicomponent heterostructures to advance the practical application of low-bias, solar-driven ammonia synthesis.

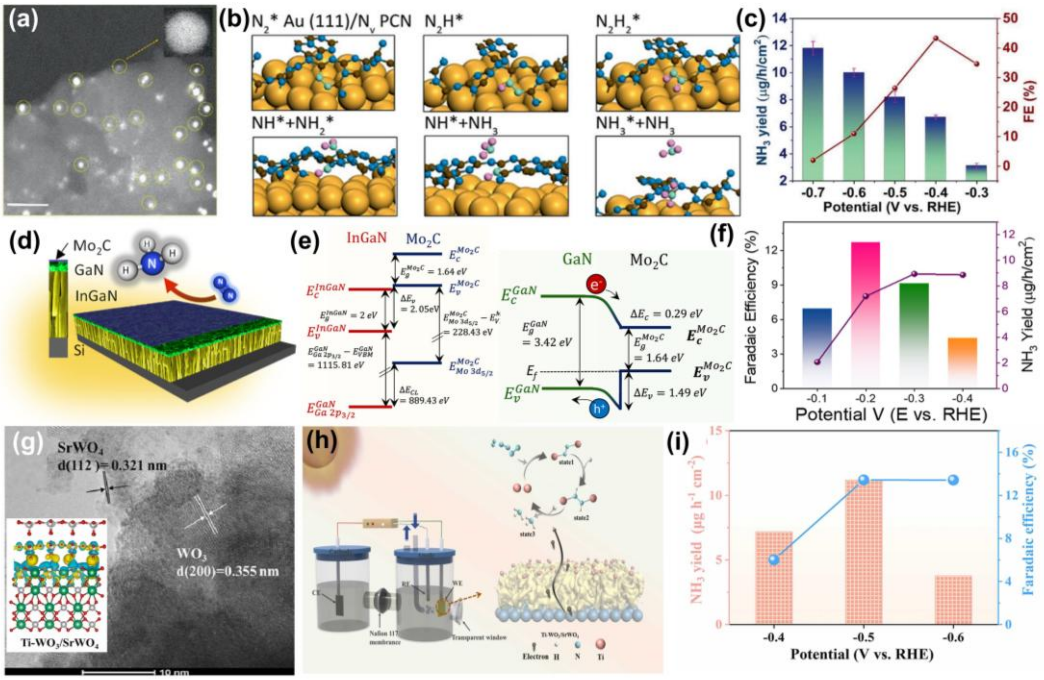

Figure 5. (**a**) HRTEM images of Au/PCN. (**b**) Zoomed tilted view of the surface where the hydrogen attacks the N_2 to show the optimized geometries of the reaction intermediates. (**c**) Schematic illustration of the Au/PCN catalyst synthesis route: the porous CN was prepared via acid exfoliation process and Au loading was accomplished by chemical reduction method [65]. Copyright 2021, Wiley. (**d**) Schematic of Mo_2C/GaN/InGaN NWs for PEC N_2 reduction. (**e**) Energy band diagram of InGaN/Mo_2C and chematic representation of charge transfer from GaN to Mo_2C. (**f**) Graphical representation of FE and NH_3 yield of Mo_2C/GaN/InGaN NWs at various applied potentials vs RHE [66]. Copyright 2023, American Chemical Society. (**g**) TEM image of Ti-WO_3/$SrWO_4$; (**h**) Mechanistic diagram of ammonia synthesis by TiWO_3/$SrWO_4$. (**i**) Ammonia formation rates on 2 h reaction [67]. Copyright 2023 Elsevier.

3.1.5. Metal-Mediated Regulation

In photoelectrochemical reactions, in addition to optimizing the electrode material itself, optimizing the ion transport characteristics of the electrolyte is also a feasible way to improve overall catalytic activity. Metal-mediated electrolyte modulation is a strategy that involves introducing metal ions or soluble metal compounds into the electrolyte in dissolved and dispersed forms to regulate the chemical environment of the electrolyte and the characteristics of the interfacial reaction [68]. Its function is that metal ions can improve the solubility and activation of N_2 molecules through coordination, regulate the double-layer structure of the electrode/electrolyte interface, promote charge transfer, and simultaneously inhibit the adsorption and reduction of H^+ on the electrode surface, thereby improving the ammonia yield and Faraday efficiency of the NRR. In addition, some metal ions can stabilize the electrolyte system and reduce the generation of reaction byproducts [69].

As is shown in Figure 6a, lithium metal-mediated modulation was taken as the core innovative strategy by Huang's research work [70]. By constructing a PEC system of "p-type silicon photocathode/Li^+ medium /nonaqueous electrolyte", it broke through the key bottlenecks of traditional aqueous nonaqueous ammonia synthesis, such as low N_2 solubility, serious HER competition, and low Faraday efficiency, and realized the high-efficiency synthesis of ammonia. It is the first combination of lithium metal-mediated mechanism and silicon photocathode. With silicon as the light absorbing layer, in the tetrahydrofuran electrolyte containing 0.2 M $LiBF_4$, the electrons generated by the light will drive the reduction of Li^+ into lithium metal, which will trigger lithium-mediated N_2 reduction cycle. At the same time, the solid electrolyte interphase (SEI) layer formed by electrolyte decomposition can be used to modulate the lithium deposition behavior. The principle of metal-mediated regulation is reflected in the synergistic modulation of the lithium metal-mediated effect and the SEI layer. Under light irradiation, the photogenerated electrons of the silicon photocathode reduce the overpotential for lithium reduction. Lithium metal reacts spontaneously with N_2 to form Li_3N intermediates, and then Li_3N reacts with ethanol-provided H^+ to form NH_3 and release Li^+, resulting in the catalytic cycle of "$Li \rightarrow Li_3N \rightarrow Li^+$". (Figure 6b) The LiF component in the SEI layer in the SEI layer can promote the uniform deposition of lithium and inhibit electrolyte degradation. At the same time, the non-aqueous THF electrolyte improves the solubility of N_2, prevents the excessive contact between H^+ and the active site, and significantly inhibits the HER. This design effectively solves the problems of difficult activation of N_2, low FE due to the competition for the HER, and slow kinetics of the reaction in the conventional NRR. The ammonia yield reached 52.4 μg h^{-1} mg^{-1} with FE as high as 95% under −5 V vs Ag/Ag^+ and simulated solar irradiation conditions. (Figure 6c) This validates the effectiveness of the lithium-mediated mechanism and provides an important reference for the application of metal-mediated regulation in the design of efficient PEC NRR systems.

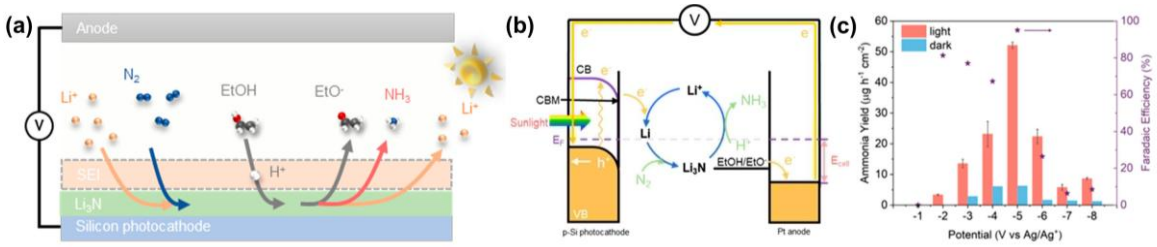

Figure 6. (**a**) Schematic illustration of lithium-mediated photoelectrochemical reduction of N_2 into NH_3 on the Si photocathode via the catalytic recycling of Li → Li_3N → Li^+, while ethanol provides the protons for the NH_3 synthesis. [70] (**b**) Schematic diagram of the PEC Li-NRR mechanism of the Si photocathode under light irradiation. [70] (**c**) NH_3 yield rates and Faradaic efficiencies of electrocatalytic Li-NRR and PEC Li-NRR process under dark (blue bars) and light (red bars) conditions [70]. Copyright 2023, American Chemical Society.

In future, the matching of metal ion types and electrolyte components can be optimized to improve the reaction kinetics; the precise regulation strategy of the SEI layer composition can be explored to further improve the stability of the system; and the combination of the metal-mediated electrolyte and the high-efficiency photoelectrode can be promoted to push the PEC NRR toward the low-bias, high FE green ammonia synthesis on a large scale.

3.1.6. Summary

Recent advances in PEC nitrogen reduction have established a multidimensional framework for performance enhancement, with targeted strategies addressing the key bottlenecks of traditional systems. These approaches

range from innovative material designs to precise atomic-level modifications, each contributing to improved activity, selectivity, and stability.

In future, the field may evolve along several synergistic pathways: integrating complementary strategies such as defect engineering with single-atom modification or combining porous COF architectures with tailored electrolyte environments; enhancing kinetics to lower overpotentials while replacing precious metals with earth-abundant alternatives; and advancing system durability and scalability under realistic operating conditions. By coupling these material and process innovations with renewable energy sources, nitrogen reduction technology can move toward green, scalable, and economically viable ammonia synthesis, supporting a sustainable industrial nitrogen cycle under the "dual-carbon" framework.

3.2. Nitrogen Oxides Reduction Reaction (NORR)

Nitrogen oxides (NO_x), prevalent in aquatic environments, represent not only a source of environmental pollution and a threat to human health but also a potential feedstock for conversion into value-added products such as ammonia. Traditional treatment and synthesis routes, however, are often hindered by high energy consumption and low efficiency. Conventional thermocatalytic processes require high-temperature for activating the reaction, leading to risks of catalyst sintering, deactivation, and substantial energy input. In contrast, PEC nitrogen oxide reduction reaction (NORR) can proceed under mild conditions by synergistically utilizing light and electrical energy [71]. This approach employs photogenerated charge carriers to drive the reduction process, while an applied bias facilitates charge separation via an external circuit to suppress recombination and backward reactions. Furthermore, localized energy input at the electrode-electrolyte interface enhances reactant activation efficiency and refines product selectivity. Collectively, these features endow PEC NORR with the dual advantages of being an environmentally benign, low-energy process and a highly efficient conversion pathway [72].

The reaction equation is as follows:

$$N_2 + 6H_2O \rightarrow 2NO_3^- + 12H^+ + 10e^-$$

3.2.1. Hydroxide/Layered Double Hydroxide (LDH) Modification

In PEC NORR, hydroxide/layered double hydroxide (LDH) were widely used to enhancing catalytic performance [73]. LDHs possess excellent intrinsic properties due to their layered structure with exchangeable interlayer anions, tunable metal cation composition, and abundant surface hydroxyl groups, resulting in high hydrophilicity and tunable electronic structure. These characteristics collectively increase the density of active sites, optimize the electronic environment for NO_x species adsorption and activation, promote the separation and transport of photogenerated charge carriers, and improve the chemical stability and corrosion resistance of the electrode. Therefore, by constructing hydroxide coatings, synthesizing LDH composites, or introducing defects into the LDH structure, the reaction efficiency, product selectivity, and energy efficiency of NORR can be significantly improved [74]. For example, a composite photocathode comprising a $Ni(OH)_2$ layer on nickel foil with a full-back-contact silicon architecture was developed by the Jin's group [75]. The nickel foil undergoes spontaneous oxidation in alkaline electrolyte to form a $Ni(OH)_2$ surface layer. (Figure 7a) Ni^{2+} sites act as Lewis acidic centers, strengthening nitrate adsorption while moderating hydrogen adsorption to suppress the HER. Furthermore, the full-back-contact design places all electrical contacts on the rear side, eliminating optical shading by the catalyst and thus maximizing light absorption. (Figure 7b) The $Ni(OH)_2$ surface layer addresses the trade-off between light harvesting and catalytic activity, achieving an NH_3 production rate of 2468 μg cm^{-2} h^{-1} with a Faradaic efficiency of 85% at −0.1 V vs. RHE. In an unbiased configuration, the system maintained a solar-to-ammonia conversion efficiency of 3.8% with stable performance over multiple cycles.

Beyond monometallic LDHs, polymetallic LDHs have garnered increasing attention for PEC NORR. The layered architecture of polymetallic LDHs with positively charged interlayers enables physical pre-enrichment of NO_x, while the multi-metal sites offer tunable active sites for adsorption and catalysis. By regulating the ionic composition and layered structure of polymetallic LDHs, the NORR activity and selectivity of can be adjusted. A representative design is illustrated in the work by Bai and colleagues, which integrated a $Fe^{2+}/Cu^{2+}/Fe^{3+}$-LDH with a $BiVO_4$ photoanode [76]. (Figure 7c) The Fe^{2+} sites act as Lewis acid centers for the chemisorption of nitrate, whereas Fe^{3+} and Cu^{2+} ions coordinate with protons to form Cu^{2+}–H/Fe^{3+}–H intermediates. These intermediates serve as a proton reservoir for NH_3 formation while simultaneously suppressing the competing hydrogen evolution reaction. This synergistic effect combining physical enrichment and chemisorption addresses the problems of limited nitrate affinity and poor selectivity commonly found in single-component semiconductors. (Figure 7d) Under an

applied potential of 0.4 V vs. RHE, the electrode delivered an NH_3 production rate of 13.8 μg cm^{-2} h^{-1} with a Faradaic efficiency of 66.1%, minimal nitrite by-product formation, and excellent cycling stability. (Figure 7e)

Theoretically, the NO_x adsorption capacity and charge transport efficiency of LDH-based cocatalysts can be optimized through multi-element doping and interlayer modulation, and the catalyst's durable can be extended by combining it with a stable substrate. By exploring the fusion of the advantages of these two strategies, PEC photocathodes suitable for different scenarios can be developed, advancing the technological realization of nitrogen oxide resource recovery and green ammonia synthesis, and contributing to pollution control and the development of new energy fields. Simultaneously, it is necessary to strengthen the research on reaction mechanisms and utilize in-situ characterization techniques to guide material design, in order to further improve the efficiency, selectivity, and stability of NORR catalysts.

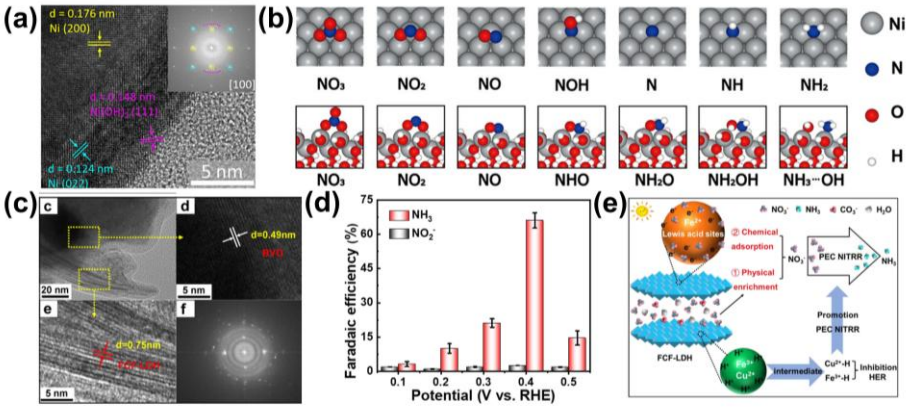

Figure 7. (**a**) HRTEM images of $Ni(OH)_2$/Ni interface. (**b**) Optimized structures of the NO_3RR on the Ni (top) and $Ni(OH)_2$ (bottom) [75]. Copyright 2025, Wiley. (**c**) HRTEM image of FCF-LDH/BVO. (**d**) The FE of FCF-LDH/BVO. (**e**) Schematic diagram of mechanism of FCF-LDH/BVO used in PEC NORR [76]. Copyright 2025, Elsevier.

3.2.2. Metal-Sites Modification

Decorating metal sites on semiconductor surfaces represents a powerful strategy to tailor the interfacial properties and catalytic activity in PEC NORR. By creating well-defined metal-active sites, these modifications directly regulate the local electronic structure, optimize the adsorption energetics of nitrate and reaction intermediates, and steer the reaction pathway away from competing processes such as HER [77,78].

Bimetallic or multimetallic alloy nanoparticles offer a powerful means to combine and enhance the properties of constituent metals. This is exemplified in systems utilizing CoCu alloy nanoparticles as surface modifiers. In one prominent study as is shown in Figure 8a, a CoCu-decorated TiO_2/Sb_2Se_3 architecture was developed, where the alloy particles served as the primary catalytic engine [79]. As is demonstrated in Figure 8b,c, the electronic synergy between Co and Cu atoms within the alloy creates active sites that effectively adsorb and activate nitrate ions, mimicking the performance of more expensive noble metals while improving stability. This approach directly addresses the poor inherent catalytic activity of the underlying Sb_2Se_3 absorber, leading to a high NH_3 Faradaic efficiency of 88.01% and a positively shifted reaction onset potential.

Noble metal nanoparticles, particularly gold (Au), remain benchmark modifiers due to their exceptional catalytic activity and favorable redox properties. A key advancement in this area involves the integration of uniformly sized Au nanoparticles with ordered silicon nanowire (O-SiNW) arrays [80]. (Figure 8d) The Au nanoparticles are not merely adjuncts but the critical active components responsible for nitrate reduction via a dynamic Au^0/Au^+ redox cycle. The ordered nanowire substrate ensures optimal light harvesting and mass transport, while the well-dispersed Au nanoparticles provide a high density of efficient and regenerable catalytic sites. This synergy enabled the system to achieve a record Faradaic efficiency of 95.6%, demonstrating the peak performance attainable with optimized noble metal modifiers.

Beyond existing alloys and precious metals, the future of metal site modification lies in expanding the library of active components. This involves developing modified materials that offer unique electronic structures and binding properties while reducing costs without compromising activity. Furthermore, designing multi-component modifier systems where different metals or compounds play complementary roles, such as sequential adsorption, activation, and proton transfer, provides pathways to unleash superior synergistic effects. Simultaneously, advancing deposition

and anchoring methods is crucial for ensuring strong adhesion, uniform distribution, and long-term operational stability of various metal modifiers, which is essential for developing practical and scalable PEC NORR.

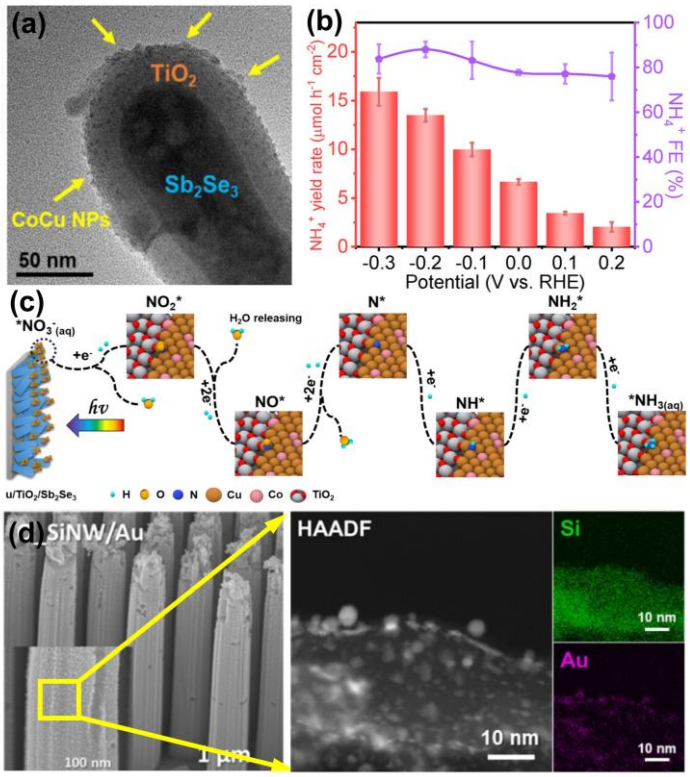

Figure 8. (**a**) TEM images of CoCu/TiO_2/Sb_2Se_3. (**b**) NH_4^+ FEs and yield rates of CoCu/TiO_2/Sb_2Se_3 in various applied potentials. (**c**) Main reaction pathway of NO_3^- reduction to ammonia on CoCu/TiO_2/Sb_2Se_3 photocathode [79]. Copyright 2024. Wiley. (**d**) HAADF-STEM and EDS mapping (Si and Au) of O_SiNW/Au [80]. Copyright 2022. Wiley.

3.2.3. Bandgap Engineering

Band structure engineering essentially involves constructing customized electronic structures by coupling interfaces between different materials, which is crucial for efficient PEC NORR [81]. The core features of such heterojunctions lie in band bending and the formation of a built-in electric field at the interface. This built-in electric field drives the spatial separation of photogenerated electron-hole pairs, suppresses their recombination, and provides a directional force for charge transport to catalytic sites [82]. Furthermore, by combining materials with complementary light absorption properties, the utilization range of the solar spectrum can be broadened. Ultimately, the synergistic effect at the heterojunction interface optimizes the electronic structure of the active sites, enhances nitrate adsorption and activation, and suppresses competing reactions such as the hydrogen evolution reaction (HER), thereby improving overall catalytic efficiency, selectivity, and durability [83,84].

Integrating organic semiconductors with inorganic catalysts is a promising route to decouple and optimize light-harvesting and catalytic functions through band alignment. A notable example is given in Figure 9a. A system combining an organic semiconductor light-absorber with a Ni-Fe-P catalyst layer on a copper foil substrate was reported by Lee's group [85]. The organic semiconductor layer is selected for its broad spectral absorption, while the Ni-Fe-P layer, whose electronic state is modulated by phosphorus, provides optimized $Ni^{\delta+}$/$Fe^{\delta+}$ active sites. The key to its function lies in the band alignment at the organic/inorganic interface, which facilitates charge injection from the organic semiconductor absorber into the catalytic layer. This heterostructure design overcomes the typical instability of organic semiconductor electrodes, achieving a notable NH_3 Faradaic efficiency of 95.6% under unbiased conditions. (Figure 9b)

Silicon, with its excellent optoelectronic properties, often serves as a foundational light absorber, but its performance hinges on effective interfacial band engineering to mitigate corrosion and facilitate charge transfer. This is exemplified in a tandem "Cu-C/Si-TiO_2" heterojunction system [86]. (Figure 9c) In this architecture, a Schottky junction formed between silicon and a carbon layer decorated with Cu nanoparticles promotes the

extraction of silicon's photogenerated electrons to surface Lewis acid sites. (Figure 9d) Concurrently, a TiO_2 photoanode with a compressively stressed interface improves charge separation. The precise band alignment across this multi-interface system addresses silicon's vulnerability in alkaline media, resulting in an NH_3 yield of 115.3 μg cm^{-2} h^{-1} with 88.8% Faradaic efficiency. (Figure 9e)

Constructing heterojunctions between different metal oxides allows for fine-tuning of the built-in electric field and surface energetics. As is shown in Figure 9f,g, a representative case is a Si/Cu-NSTL/$Co(OH)_2$ ternary photocathode, where a nanostructured copper layer is integrated with $Co(OH)_2$ nanosheets [87]. The intimate interface between Cu and $Co(OH)_2$ establishes a strong built-in electric field that not only accelerates charge separation but also promotes the co-adsorption of nitrate and water molecules, critically suppressing HER. This band-structure-driven design tackles the limited active sites and intermediate desorption issues of conventional photocathodes, achieving near-unity Faradaic efficiency for NH_3 at 1.0 V vs. RHE. Similarly, a CeO_2-C/$BiVO_4$ composite leverages the heterojunction between p-type $BiVO_4$ and CeO_2 to induce beneficial band bending [88]. The incorporated carbon layer further modulates the interface, enhancing electron transfer. This coordinated band engineering significantly suppresses charge recombination and leads to an NH_3 Faradaic efficiency of 32.2% with excellent operational stability.

Future advancements in heterostructure design will likely focus on exploring novel material combinations with more sophisticated band alignment. This includes developing multi-component heterostructures to achieve synergistic broad-spectrum response and high catalytic site density. Deepening the understanding and precise control of interfacial band bending in tandem or ternary junctions will be key to minimizing charge-transfer losses. For practical application, strengthening in situ characterization of interfacial charge dynamics and active site evolution under operating conditions will provide the essential theoretical foundation for designing the next generation of efficient, stable, and scalable PEC NORR systems.

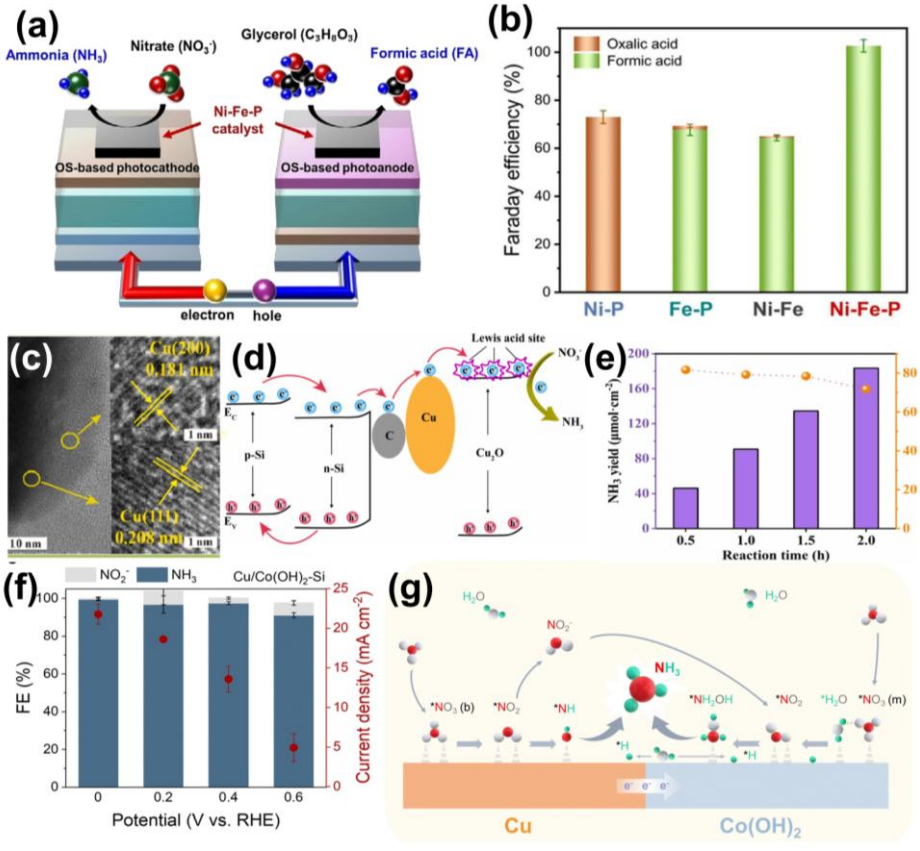

Figure 9. (**a**) Schematic illustration of a bias-free PEC upcycling system designed for the simultaneous conversion of nitrate to ammonia and glycerol to formic acid. (**b**) Faradaic efficiency for products by GOR at 10 mA cm^{-2} [85]. Copyright 2025. Wiley. (**c**) HRTEM images of CuCSi-800 focusing on a certain Cu NP. (**d**) Schematic representation of the work mechanism for PEC NORR on the CuCSi-800. (**e**) Time dependence of NH_3 yield (purple column diagrams) and FE (orange point plots) obtained from CuCSi-800 [86]. Copyright 2024. Elsevier. (**f**) FE of Cu/$Co(OH)_2$–Si under different applied potentials in NORR. (**g**) Schematic representation of the proposed NORR catalytic mechanism in Cu/$Co(OH)_2$–Si and the synergetic effect between Cu and $Co(OH)_2$ [87]. Copyright 2024. The Royal Society of Chemistry.

3.2.4. Defect Engineering

The deliberate introduction of defects into semiconductor materials, such as vacancies, interstitial atoms, and heteroatom dopants， serves as a precise method to modulate electronic band structures for enhanced PEC NORR [89]. Defect states within the bandgap can act as charge-trapping centers, prolonging carrier lifetimes and promoting separation, thereby increasing the flux of photogenerated electrons available for nitrate reduction [90]. Beyond charge dynamics, these defects directly alter the surface electronic state, which can optimize the adsorption energetics of nitrate ions and key intermediates as $*NO_2$ while simultaneously moderating hydrogen adsorption to suppress the competing HER [91]. Furthermore, defect-induced band tailing or the creation of mid-gap states can effectively narrow the optical bandgap, broadening the spectral response. Collectively, strategic defect engineering enhances light harvesting, charge separation, and surface catalysis, leading to improved activity, selectivity, and stability in NORR systems.

Introducing oxygen vacancies (V_O) is a prevalent strategy to tune both the bulk and surface electronic structure of metal oxides. A representative application is demonstrated in Figure 10a, it is found in work on Cu_2O photocathodes for the co-reduction of CO_2 and nitrate to urea [92]. Here, controlled creation of surface oxygen vacancies induces a reconstruction of copper valence states, generating a mixed $Cu^0/Cu^+/Cu^{2+}$ environment. Critically, these vacancies modify the local band structure, shifting the conduction band minimum to a more negative potential that thermodynamically facilitates both CO_2 and nitrate reduction. The defect-mediated surface also enhances the adsorption of both reactants. Introducing oxygen vacancies can achieve dual regulation of electronic structure and active sites, enabling efficient C-N coupling reactions under mild conditions to accommodate complex multi-reactant reduction pathways.

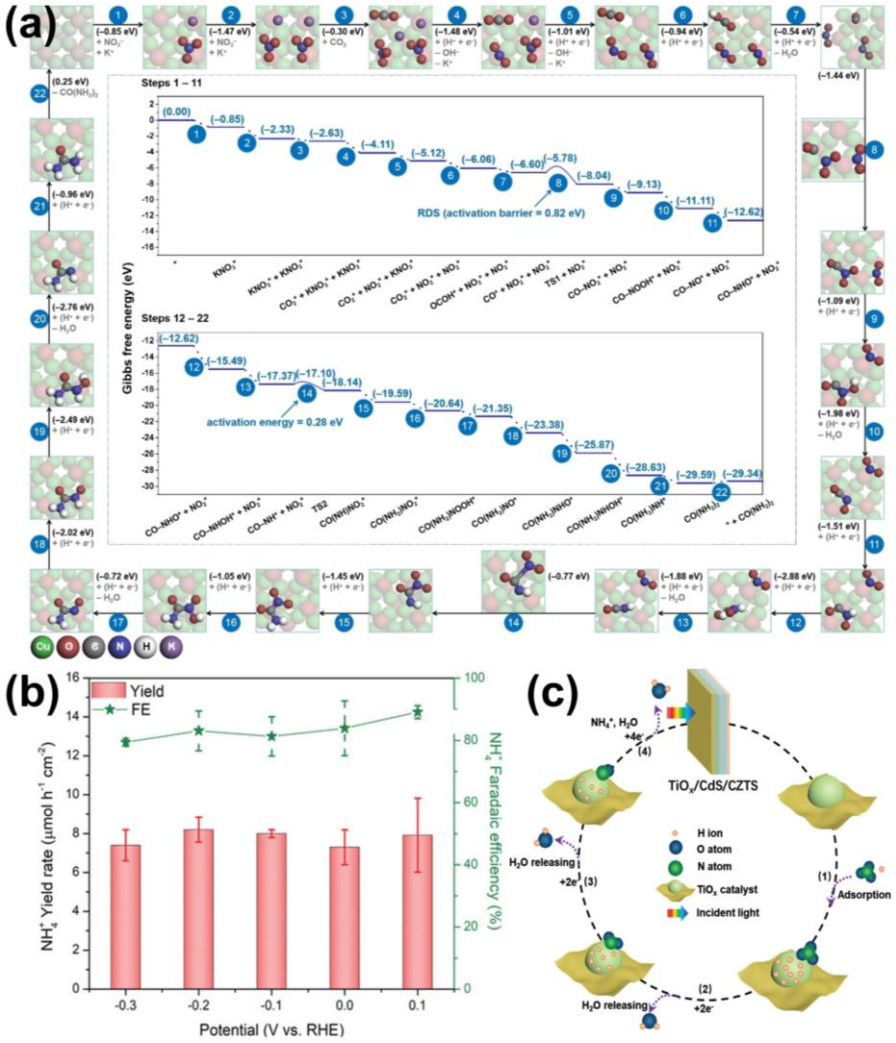

Figure 10. (**a**) Theoretical studies of the reaction mechanism of PEC co-reduction of CO_2 and NO_3^- to urea on Cu_2O (100) facet at reaction conditions [92]. Copyright 2024. Wiley. (**b**) NH_4^+ Faradaic efficiency and yield rate of TiO_x-250/CdS/CZTS in different applied potentials. (**c**) Proposed reaction pathway of NO_3 reduction to ammonia on TiO_x/CdS/CZTS photocathode [93]. Copyright 2022. Wiley.

Doping with lower-valence cations or creating cation deficiencies introduces defect states that can enhance conductivity and create specific adsorption sites. This approach is exemplified in a defect-engineered TiO_x/CdS/chalcopyrite photocathode [93]. As shown in Figure 10b,c, by rationally controlling the spray pyrolysis temperature, the concertration of Ti^{3+} species which acting as donor defects in the TiO_x layer was regulated. These Ti^{3+} defects create intra-bandgap states that improve charge separation and transport across the heterojunction. More importantly, they serve as preferential adsorption sites for nitrate and its reduction intermediates, steering the reaction pathway and suppressing undesirable side reactions. This defect-mediated optimization of both charge kinetics and surface chemistry led to a high Faradaic efficiency for ammonia of 89.1% at 0.1 V vs. RHE with notable retention in complex simulated wastewater.

Future advances in defect engineering for PEC NORR will focus on achieving even more precise and tailored control over the electronic landscape. This includes developing synthetic protocols to selectively generate specific defect types including anion/cation vacancies and targeted dopants at desired concentrations and spatial distributions to optimally align with the energetic requirements of nitrate reduction. Combining defect engineering with other material strategies, such as constructing heterojunctions where defects are localized at critical interfaces, could achieve synergistic effects for superior charge management and catalytic specificity. For practical deployment, enhancing the stability of these defect sites under operational conditions in real wastewater matrices is crucial. Concurrently, employing in situ and operando characterization techniques will be vital to elucidate the dynamic evolution of defect states and their interaction with reactants under working conditions, providing a fundamental roadmap for the rational design of next-generation defect-engineered PEC systems.

3.2.5. Summary

Nowadays, the core challenge on PEC NORR lies in designing materials that can efficiently harvest light, generate long-lived charge carriers, and provide surface sites with optimized energetics for the selective multi-electron reduction of nitrate to ammonia, while suppressing competing pathways such as the hydrogen evolution reaction HER. To address this, several interconnected material modification strategies have emerged as central to performance enhancement, each targeting specific aspects of the electronic and interfacial structure.

Typical material optimization approaches focus on strategically altering the band structure and interfacial charge dynamics. Defect engineering, through the introduction of vacancies or dopants, creates intra-gap states that can enhance visible-light absorption, trap charge carriers to reduce recombination, and tailor surface electronic properties for improved nitrate adsorption. Heterojunction construction couplling materials with complementary band alignments to generate a built-in electric field, which forcefully separates photogenerated electrons and holes and directs them toward desired reaction interfaces. Surface modification with metal-based sites introduces localized states that act as efficient catalytic centers, lowering the activation barrier for nitrate reduction and modulating intermediate binding energies to steer product selectivity.

Despite significant progress, several critical challenges must be resolved to advance PEC NORR toward practical application. A primary issue is the inefficient spatial and energetic management of charge carriers, leading to substantial losses through bulk and surface recombination before they can participate in catalysis. Furthermore, achieving high selectivity for ammonia over other nitrogenous byproducts such as nitrite or HER remains difficult, as it requires exquisite control over the multi-step proton-coupled electron transfer process. Material stability under prolonged operation in often corrosive electrolytes is another persistent concern, as photo-corrosion and catalyst degradation limit system longevity. Finally, many high-performance strategies currently rely on scarce or costly elements, creating a need to develop equally effective systems based on earth-abundant materials.

Therefore, future development must will focus on the precise integration of multiple band-engineering strategies. This involves moving beyond singular modifications toward composite designs, such as combining defect-engineered absorbers with tailored heterojunctions and atomically dispersed catalytic sites, to create synergistic effects that simultaneously maximize light absorption, charge separation, surface reactivity, and operational stability. Advancing in-situ and operando characterization techniques will be crucial to elucidate the dynamic interplay between the engineered electronic structure and the catalytic mechanism under working conditions. Success in these areas will pave the way for designing efficient, durable, and scalable PEC systems for sustainable nitrate valorization.

4. Photoanode Valorization Conversions

In photoelectrochemical (PEC) systems, the photoanode has traditionally been employed to drive the oxygen evolution reaction (OER) via water oxidation. In pursuit of higher energy efficiency and product value, research has expanded toward alternative anodic reactions that generate more valuable products or coupled fuels. Among

these, the urea oxidation reaction (UOR) and the selective alcohols oxidation reaction have garnered significant attention [94–96]. UOR offers the dual benefit of degrading an environmental pollutant while producing hydrogen at a significantly lower thermodynamic potential than OER, thereby reducing the overall energy input for hydrogen generation [97]. Concurrently, the PEC alcohols oxidation presents a route to directly synthesize high-value organic intermediates under mild conditions [98].

The efficient and value-added conversion of feedstocks like urea and alcohols in conventional chemical production faces distinct challenges. For UOR, the six-electron transfer process is kinetically sluggish and often suffers from incomplete oxidation to N_2 and CO_2, with competing side reactions generating harmful intermediates like nitrite [94]. Similarly, traditional methods for alcohol oxidation, including thermal catalysis, often require harsh conditions, exhibit limited selectivity, and entail difficult product separation, particularly for converting structurally similar polyols [99–101].

PEC photoanode valorization conversions offer a promising platform to address these challenges. For UOR, the application of a light-active anode can provide photogenerated holes with high oxidative potential to drive the complex C-N bond cleavage, while the applied bias facilitates charge separation and suppresses recombination [102]. In parallel, for alcohol oxidation, this technology enables selective reactions at ambient temperature and pressure by precisely steering reaction pathways through modulation of applied potential and light irradiation [103]. By optimizing the band structure of photoanode materials and enhancing interfacial charge-transfer efficiency, PEC systems can promote target pathways, whether for complete urea degradation or selective alcohol oxidation, while significantly suppressing competing side reactions [104]. The applications of these alternative oxidations are substantial. UOR is pivotal for wastewater treatment and energy-saving hydrogen production when integrated with cathodic HER [105]. Meanwhile, alcohols serve as important platform molecules for valorization. Selective oxidation of methanol and ethylene glycol can yield high-value intermediates like formaldehyde and glycolic acid [106–108]. Biomass-derived polyols can be oxidized to fine chemicals, and aromatic alcohols find applications as oxidized derivatives in pharmaceuticals and fragrances [109,110].

However, key challenges remain. For both UOR and alcohol oxidation, achieving high selectivity and Faradaic efficiency for the desired products is difficult due to complex multi-step mechanisms and competing over-oxidation or mineralizing pathways. The development of cost-effective, stable, and highly active photoanode materials that can selectively stabilize key reaction intermediates is a central research focus [111,112]. Furthermore, understanding and mitigating catalyst deactivation under operational conditions is critical for long-term application.

In the following sections, the mechanisms, material design strategies, and progress for these value-added anodic reactions will be discussed in detail.

4.1. Urea Oxidation Reaction

In PEC systems, the photoanode has traditionally been dedicated to driving OER. To pursue reactions with higher energy efficiency and economic value, alternative anodic oxidations that yield valuable products have gained significant attention. Among these, UOR stands out as a promising pathway that aligns with the dual objectives of pollution control and resource recovery.

The motivation for developing UOR technology stems from severe environmental and resource challenges. Excessive use of nitrogen fertilizers, discharge of domestic sewage, and industrial by-products have led to the widespread accumulation of urea in water bodies, causing eutrophication and threatening aquatic ecosystems [113]. Concurrently, urea, a molecule containing both nitrogen and hydrogen, represents a potential chemical resource for the synthesis of valuable products like ammonia or hydrogen. However, conventional catalytic methods for urea conversion are often hampered by high energy consumption, poor environmental adaptability, and inefficient resource utilization [114].

In contrast, PEC UOR offers a compelling alternative for urea valorization at the photoanode. It operates under mild conditions, can be directly powered by solar energy or renewable electricity, and demonstrates high selectivity for desired products along with strong environmental compatibility. This approach enables a synergistic pollution control and resource production strategy, effectively overcoming the limitations of traditional catalysis and establishing itself as a preferred direction for efficient urea conversion and environmental remediation.

4.1.1. Heterostructure Construction

The construction of heterostructures represents a sophisticated strategy for band-structure engineering in PEC UOR. By interfacing inorganic semiconductors with organic conjugated polymers, a hybrid system with a tailored electronic landscape is created. The core function of such a design is to establish favorable interfacial band alignment, typically a type-II heterojunction—which generates a built- in electric field to drive the spatial

separation of photogenerated charge carriers [115]. This strategy directly addresses the critical limitations in UOR, such as rapid charge recombination and inefficient visible-light utilization [116]. Furthermore, the synergistic interaction at the hybrid interface can optimize the adsorption and activation of urea molecules, suppress competing side reactions, and enhance the overall catalytic stability, thereby providing a fundamental material platform for efficient and integrated energy conversion and pollution remediation.

This mechanism of band-structure modulation via hybrid interfaces is effectively demonstrated in specific material systems [117]. As is demonstrated in Figure 11a, work by Bezboruah and colleagues designed a composite system of nickel-doped TiO_2 (Ni-TiO_2) nanorods/thiophene-naphthalene diimide copolymer (p-NDIHBT) [118]. In this system, the wide-bandgap TiO_2 is chemically modified and coupled with a narrow-bandgap organic polymer. Their integration forms a type-II heterojunction, which results in a staggered band alignment that not only extends the spectral response into the visible region but also facilitates the directional flow of photogenerated electrons and holes across the interface, thereby mitigating recombination. (Figure 11b) This deliberate band engineering overcomes the poor visible-light absorption of pristine TiO_2 and the limited charge transport of the organic polymer alone. As a result, the optimized heterostructure achieved a notable Faradaic efficiency of 83.3% for the coupled hydrogen evolution reaction and maintained stable performance during operation, underscoring how targeted interfacial design can unlock synergistic gains in activity and stability.

By rationally designing the structure of modified heterojunctions, the catalytic activity of the heterojunctions can be further optimized. The fabrication of core shell and multilayer heterojunctions constitutes a precise method for engineering advanced heterostructures in photoelectrochemical urea oxidation systems. This design strategy integrates materials with distinct functions: a core component typically provides essential properties such as electrical conductivity or structural support, while the surrounding shell or additional layers introduce tailored catalytic, optical, or protective functionalities. The primary advantage of such architectures stems from the well-defined interfacial interactions and synergistic coupling between the different layers. This integrated approach collectively enhances charge separation, extends light absorption, regulates surface reaction pathways, and improves long term catalyst stability. By spatially organizing multiple functional components, core shell and multilayer designs effectively address common limitations in conventional systems, including high charge recombination rates, slow reaction kinetics, limited product selectivity, and insufficient operational durability.

As is shown in Figure 11c, a clear illustration of this design principle is provided by work on photoanodes consisting of one-dimensional SnO_2-$BiVO_4$/Co-Pi core shell nanorod arrays [119]. A visible light responsive $BiVO_4$ shell layer extends the spectral absorption range and supplies active sites for oxidation reactions. An outermost Co-Pi cocatalyst layer further accelerates the surface reaction kinetics. The interfaces between these layers are carefully engineered to establish favorable band alignments. Specifically, the SnO_2-$BiVO_4$ junction forms an n-n heterojunction that promotes electron hole separation and minimizes recombination, while the $BiVO_4$/Co-Pi interface facilitates efficient hole extraction and their conversion into active high valence cobalt species. (Figure 11d) This hierarchical structural design results in a significant negative shift of the urea oxidation onset potential and a high Faradaic efficiency for urea conversion, demonstrating how precisely structured multilayer heterojunctions can synergistically optimize charge transfer, light harvesting, and surface catalytic activity.

The rational construction of heterostructures constitutes a foundational and highly effective strategy for advancing photoelectrochemical urea oxidation systems. Its essential role is to engineer the interfacial band alignment and charge carrier dynamics between dissimilar materials, thereby directly addressing the core challenges of charge recombination, limited light absorption, and slow surface reaction kinetics. This is achieved by creating tailored electronic junctions, such as type-II heterojunctions or graded multilayer interfaces, which generate built-in electric fields to spatially separate photogenerated electrons and holes, broaden the spectral response, and provide optimized active sites for urea activation.

Future developments of heterostructure engineering will necessitate a more precise and programmable approach to interface design. Research efforts will likely focus on achieving atomic-level control over junction formation, exploring novel combinations of materials such as layered double hydroxides with conductive frameworks or integrating single-atom catalysts into multidimensional architectures. Advanced computational modeling will play an increasingly critical role in predicting optimal band alignment and synergistic effects prior to experimental synthesis. Concurrently, enhancing the long-term stability of these complex interfaces under operational conditions, including in real wastewater matrices, will be paramount for practical application. Furthermore, integrating these sophisticated heterostructures into scalable device architectures that operate efficiently under natural solar illumination and can be coupled with other renewable energy processes represents the next crucial step. By deepening the fundamental understanding of interfacial charge and mass transport through in-situ and operando characterization, and by fostering convergence between materials science, electrochemistry, and systems engineering, heterostructure strategies are poised to enable the realization of efficient, durable, and

economically viable photoelectrochemical technologies for sustainable urea valorization and integrated environmental remediation.

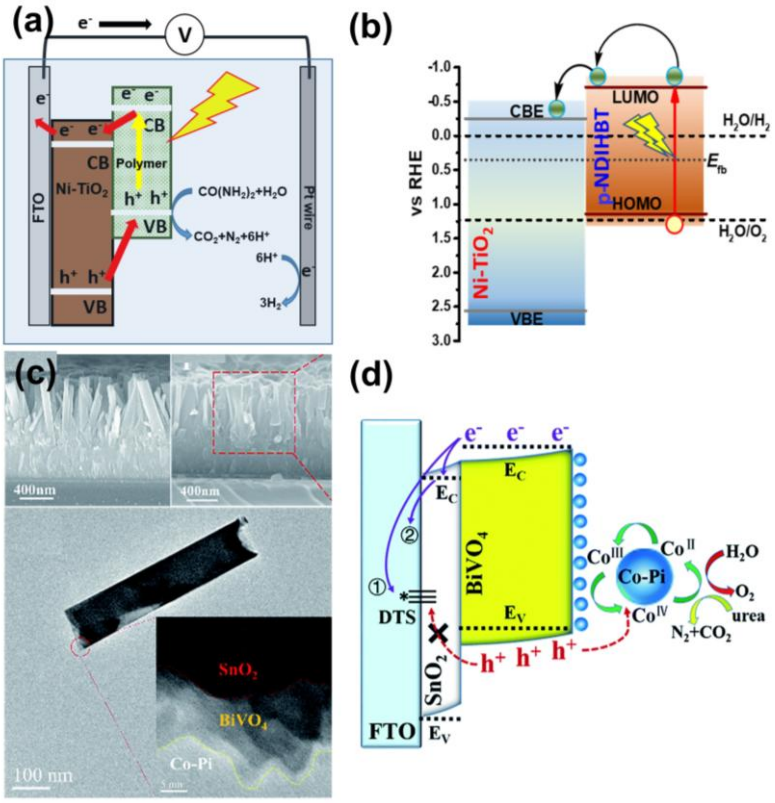

Figure 11. (**a**) Schematic reaction diagram of a photoelectrochemical cell for hydrogen production. (**b**) The expected type-II band alignment between Ni–TiO_2 and p-NDIHBT based on the flat band potentials [117]. Copyright 2022 Elsevier. (**c**) Morphology of SnO_2@$BiVO_4$/Co-Pi NRAs. (**d**) Illustration of the square box shows the energy diagram of the SnO2@BiVO4 heterojunction photoanode and illustrates the basic operation mechanism for solar driven water splitting and urea oxidation [119]. Copyright 2019. The Royal Society of Chemistry.

4.1.2. Kinetics Optimization

In PEC UOR, kinetic optimization focuses on precisely lowering the reaction activation energy and stabilizing key intermediates through tailored material design. This primarily involves two interconnected strategies: modulating the electronic structure and density of catalytic active sites to strengthen urea adsorption and activation, and steering the reaction along a favorable pathway towards the target products while suppressing undesirable side reactions. These approaches address the fundamental kinetic challenges in UOR, including the high energy barrier for C-N bond cleavage, sluggish reaction rates, and insufficient selectivity.

A proven strategy for overcoming kinetic limitations is the creation of specific active sites that alter the rate-determining step. This is effectively demonstrated as the NiO-Ni-n-Si photoanodes fabricated by Dang's group [120]. (Figure 12a) As is demonstrated in Figure 12b–d, kinetic enhancement was achieved by generating high-valence nickel-oxo species (Ni^{4+}=O) as pivotal active centers. In this work, photogenerated holes accumulate at the surface to form Ni^{4+}=O. The strong interaction between this site and the urea molecule significantly weakens the C-N bond, which possesses partial double-bond character. This interaction lowers the activation energy for bond cleavage and accelerates the overall reaction by modifying the rate-determining step. Consequently, this targeted active site engineering yielded a high Faradaic efficiency exceeding 90% for the target product and maintained notable stability under intensive illumination.

Beyond active site engineering, explicitly guiding the reaction mechanism towards a specific pathway is equally critical for kinetic optimization. The design must facilitate the formation of desired intermediates while bypassing energetically costly or unproductive routes. For instance, directing the reaction through a cyanate (NCO^-) intermediate pathway, rather than those leading to excessive nitrogen oxidation, can effectively enhance selectivity and speed for the target nitrogenous product. The synergy between a well-designed active site and a favorable reaction channel is thus paramount. Future developments will likely involve the use of advanced in-situ spectroscopy and computational simulations to precisely map these pathways. This deeper mechanistic

understanding will enable the rational design of catalytic interfaces that not only provide optimal active sites but also intrinsically guide the reaction sequence, paving the way for UOR systems with superior activity, selectivity, and energy efficiency.

4.1.3. Catalytic System Integration

In PEC UOR, kinetic optimization aims to accelerate the rate-limiting steps of both the UOR and its coupled cathodic process, while minimizing the overall energy input. This is effectively achieved by integrating a rationally designed composite catalytic system within a dual-electrode architecture [121]. Such integration enables simultaneous optimization of the anodic UOR kinetics and the kinetics of the paired cathodic reaction, typically hydrogen evolution. The core strategy involves engineering each electrode to address its specific kinetic bottlenecks—such as charge transfer resistance, active site density, and intermediate adsorption energetics—thereby creating a synergistic system where both half-reactions proceed efficiently under a shared applied bias [122].

A practical implementation of this strategy is demonstrated in Figure 12e as a dual-compartment PEC system incorporating a $Co_3O_4/BiVO_4$ heterojunction photoanode paired with a $MoNiCuO_X/Cu$ nanowire cathode [123]. The kinetic optimization at the anode is addressed through the construction of a p-n heterojunction, which establishes a built-in electric field to drastically enhance the separation and transfer of photogenerated charges. This design not only increases the flux of holes available for oxidation but also selectively promotes the generation of chloride radicals over hydroxyl radicals. This selective oxidation pathway favors the conversion of urea to nitrogen gas while suppressing over-oxidation to nitrate, thereby directly improving the reaction kinetics and selectivity for total nitrogen removal (Figure 12f).

Optimizing the kinetic matching between electrodes will be a key focus of future research in this field. This includes exploring advanced catalyst doping techniques to reduce overpotential, adjusting interfacial structures to accelerate charge transfer, and employing operational parameters such as adaptive potential control and reactant concentration management to dynamically optimize system performance under different conditions. This synergistic optimization strategy for anode and cathode kinetics provides a scalable framework for developing efficient, integrated photoelectrochemical systems that can simultaneously achieve wastewater purification and energy-positive chemical synthesis.

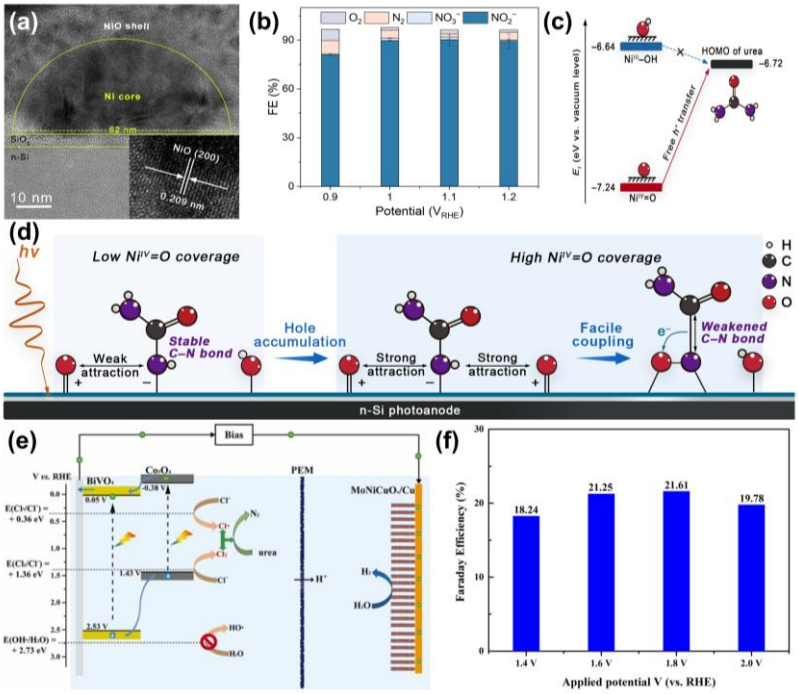

Figure 12. (**a**) HRTEM of NiO@Ni/n-Si photoanode. (**b**) Products distribution of PEC UOR using NiO@Ni/n-Si photoanode under various potentials. (**c**) Schematics of the decay process of surface-trapped holes during UOR on the NiO@Ni/n-Si photoanode. (**d**) Schematic of NiIV=O-coverage-dependent kinetics of PEC UOR on the NiO@Ni/n-Si photoanode [120]. Copyright 2025. Wiley. (**e**) Illustration of the TN removal and hydrogen

generation mechanism in the photoelectrocatalytic system induced by Co3O4/BiVO4 photoanode and MoNiCuOx/Cu cathode. (**f**) The faradaic efficiency of urea oxidation on different applied potential [123]. Copyright 2019. Elsevier.

4.1.4. Summary

The advancement of PEC UOR is fundamentally driven by deliberate band structure engineering, which governs light absorption, charge separation, and interfacial reaction kinetics. Current research focuses on designing semiconductor heterojunctions, introducing tailored defects, and applying surface modifications to construct optimal electronic interfaces. These strategies collectively address the inherent limitations of single-component systems, such as rapid charge recombination, insufficient visible-light utilization, and sluggish surface reaction dynamics.

Common performance enhancement methods center on modifying the electronic landscape of photoanodes. Constructing heterojunctions with type-II band alignment creates built-in electric fields that promote the spatial separation of photogenerated carriers. Introducing defect states within the bandgap can extend light absorption and serve as charge-trapping centers to prolong carrier lifetimes. Surface modifications with catalytic overlayers or atomic sites further tailor the interfacial energy diagram, lowering the activation barrier for urea oxidation while suppressing competing pathways. Together, these band-engineering approaches enhance photocurrent density, improve Faradaic efficiency, and increase operational stability.

Looking forward, several key challenges must be resolved to transition PEC UOR toward practical application. First, achieving precise and stable band alignment under operating conditions remains difficult, particularly in complex aqueous environments. Second, the long-term durability of engineered interfaces against photo-corrosion and fouling needs significant improvement. Third, scaling up material synthesis while maintaining fine control over band structure at low cost is essential for industrialization. Future efforts should integrate in-situ characterization with computational modeling to dynamically map interfacial energy landscapes and guide the rational design of robust, scalable photoanodes. By advancing both fundamental understanding and practical engineering of band structures, PEC UOR can evolve into an efficient technology for simultaneous wastewater remediation and sustainable chemical production.

4.2. Ammonia Oxidation Reaction

Ammonia serves as a critical nitrogen-containing feedstock for chemical synthesis, an essential reducing agent in environmental processes such as denitrification and CO_2 conversion, and a potential fuel for direct ammonia fuel cells [124]. However, conventional catalytic technologies for ammonia conversion face significant limitations: the industrial oxidation of ammonia to nitric acid requires platinum-based catalysts operating above 800 °C; selective catalytic reduction of NO_x with ammonia typically demands a temperature window of 300–400 °C and risks generating the greenhouse gas N_2O; and catalysts in direct ammonia fuel cells are often susceptible to poisoning by strong ammonia adsorption [125].

PEC ammonia oxidation reaction (AOR) offers a promising alternative by leveraging light energy to drive the reaction under mild conditions [126]. The process begins with the generation of electron-hole pairs in a semiconductor photoanode upon illumination. The photogenerated holes, which accumulate at the electrode-electrolyte interface, act as potent oxidants that can selectively convert ammonia to nitrogen-containing products such as NO_2^- or NO_3^- [112]. The reaction pathway can be tuned by adjusting the semiconductor's band structure, the applied bias, and the catalyst composition, thereby directing selectivity toward desired products and minimizing over-oxidation to gaseous nitrogen oxides. Concurrently, the photogenerated electrons can be harnessed for coupled reduction reactions, such as converting NO_2^-/ NO_3^- back to N_2, enabling an integrated oxidation-reduction cycle that enhances overall nitrogen-removal efficiency.

The applications of PEC AOR align with several sustainable technology goals. In chemical manufacturing, it provides a low-temperature route to produce nitrite/nitrate precursors. In environmental remediation, it facilitates the selective conversion of ammonia to harmless N_2 or valorized nitrogen oxyanions, complementing existing denitrification and SCR processes [127]. For energy applications, PEC systems can assist in mitigating catalyst poisoning in ammonia fuel cells by controllably oxidizing residual ammonia. By operating at near-ambient temperatures, utilizing sunlight or renewable electricity, and offering high product selectivity, PEC ammonia oxidation addresses the high energy consumption, pollutant formation, and scenario limitations inherent in conventional thermal catalysis, positioning it as a key technology for the efficient and clean utilization of ammonia in a sustainable nitrogen economy [128].

4.2.1. Cocatalyst Decoration

Research on PEC AOR remains at an early stage, with current efforts primarily focused on establishing its fundamental feasibility and elucidating the underlying reaction mechanisms. These foundational studies highlight significant potential for the technology while underscoring the broad scope for future investigation.

Initial work has successfully demonstrated the viability of PEC systems for ammonia conversion. A notable study employed an iron phosphate-decorated hematite (FePi/Fe_2O_3) photoanode to drive ammonia decomposition in an alkaline aqueous electrolyte. (Figure 13a) Under simulated solar illumination and an applied bias of 1.23 V versus the reversible hydrogen electrode (RHE), this PEC system achieved an ammonia decomposition rate of approximately 54.4% within 3 h. In contrast, control experiments using only electrocatalysis or photocatalysis under otherwise identical conditions yielded significantly lower conversion rates of 22.6% and 32.0%, respectively. (Figure 13b) This comparative result clearly indicates the synergistic advantage of coupling light and electrical energy for this reaction [129]. (Figure 13c)

The enhanced performance was attributed to the critical role of surface processes and improved charge carrier management. The proposed mechanism suggests that ammonia molecules adsorb onto the catalyst surface, where they are oxidized by photogenerated holes. The presence of the FePi co-catalyst facilitates this process by undergoing continuous oxidation, which helps suppress the recombination of photogenerated electron-hole pairs within the hematite bulk. This effective charge separation promotes the transfer of holes to the surface, thereby increasing the availability of active oxidants for adsorbed NH_3. Consequently, the PEC approach achieves efficient ammonia oxidation at a substantially lower applied potential than required for purely electrocatalytic conversion, demonstrating a clear pathway toward more energy-efficient ammonia valorization and remediation.

4.2.2. Reaction Pathway and Active Site Designing

In PEC AOR, performance is governed by two complementary design principles: the rational steering of the reaction pathway and the precise engineering of active sites. Reaction pathway design involves directing the sequence of elementary steps—from ammonia adsorption to the formation of final nitrogen-containing products—by modulating operational parameters and catalyst properties. This approach minimizes energy-wasting side reactions, such as competitive water oxidation, and enhances selectivity toward target products like nitrite or nitrate. Active site design focuses on constructing atomic or ionic centers with tailored electronic structures and coordination environments on the catalyst surface. These sites act as functional anchors that strengthen reactant adsorption, lower activation barriers, and accelerate charge transfer. Together, pathway control and site engineering synergistically ensure that AOR proceeds with high efficiency, selectivity, and stability, forming the cornerstone of advanced PEC ammonia-oxidation systems.

These principles are effectively illustrated in recent work that combines bimetallic active sites with pathway modulation. Mechanistic studies using hematite (α-Fe_2O_3) photoanodes led by Yuchao Zhang's lab have provided valuable insight into the sequence of surface reactions [130]. Research has systematically identified the primary products of AOR, including dinitrogen (N_2), nitrite (NO_2^-), and nitrate (NO_3^-), alongside oxygen from the competing water oxidation reaction (WOR). Minor intermediates such as hydrazine (N_2H_4) and nitric oxide (NO) have also been detected. The competition between AOR and WOR is governed by the relative formation of surface species: Fe–O states derived from water/hydroxide and Fe-N states arising from adsorbed ammonia. A proposed non-radical nucleophilic attack mechanism describes how ammonia interacts with high-valent iron-oxo (Fe^{IV}=O) sites to form N-O bonds, leading to nitrite and subsequently nitrate. Alternatively, Fe^{III}-NH_2 species can be oxidized by photogenerated holes to form Fe^{IV}=NH intermediates, which undergo further reactions to ultimately release N_2 or N_2H_4. This work illustrates that product selectivity can be tuned by controlling the balance between Fe-O and Fe-N surface populations. (Figure 13d)

Active site design can further modulate this balance by enhancing ammonia adsorption and activation. This mechanism is effectively demonstrated in work where trace amounts of copper ions were introduced into the electrolyte of a $BiVO_4$ photoanodes [131]. (Figure 13e) The added Cu^{2+} ions formed stable Cu–NH_3 complexes that preferentially adsorbed onto the $BiVO_4$ surface. This selective adsorption effectively outcompeted water molecules for surface sites, thereby suppressing WOR. Furthermore, the synergy between the $BiVO_4$ surface and the coordinated Cu–NH_3 complexes facilitated the cleavage of N-H bonds, accelerating the initial proton-coupled electron transfer step that is often rate-limiting in AOR. This simple yet precise modification resulted in a high Faradaic efficiency of 93.8% for ammonia oxidation, highlighting how targeted manipulation of the adsorption environment and active site micro-coordination can decisively govern the competition between AOR and WOR.

Current studies underscore that the performance of PEC AOR is dictated by the interplay between fundamental reaction pathways and the atomic-level design of catalytic interfaces. By elucidating the surface mechanisms and strategically engineering sites to favor ammonia adsorption and activation, it is possible to direct

the reaction toward desired nitrogen-containing products with high efficiency and minimal energy waste. This integrated approach provides a foundational strategy for developing advanced PEC systems for sustainable ammonia valorization and nitrogen cycle management.

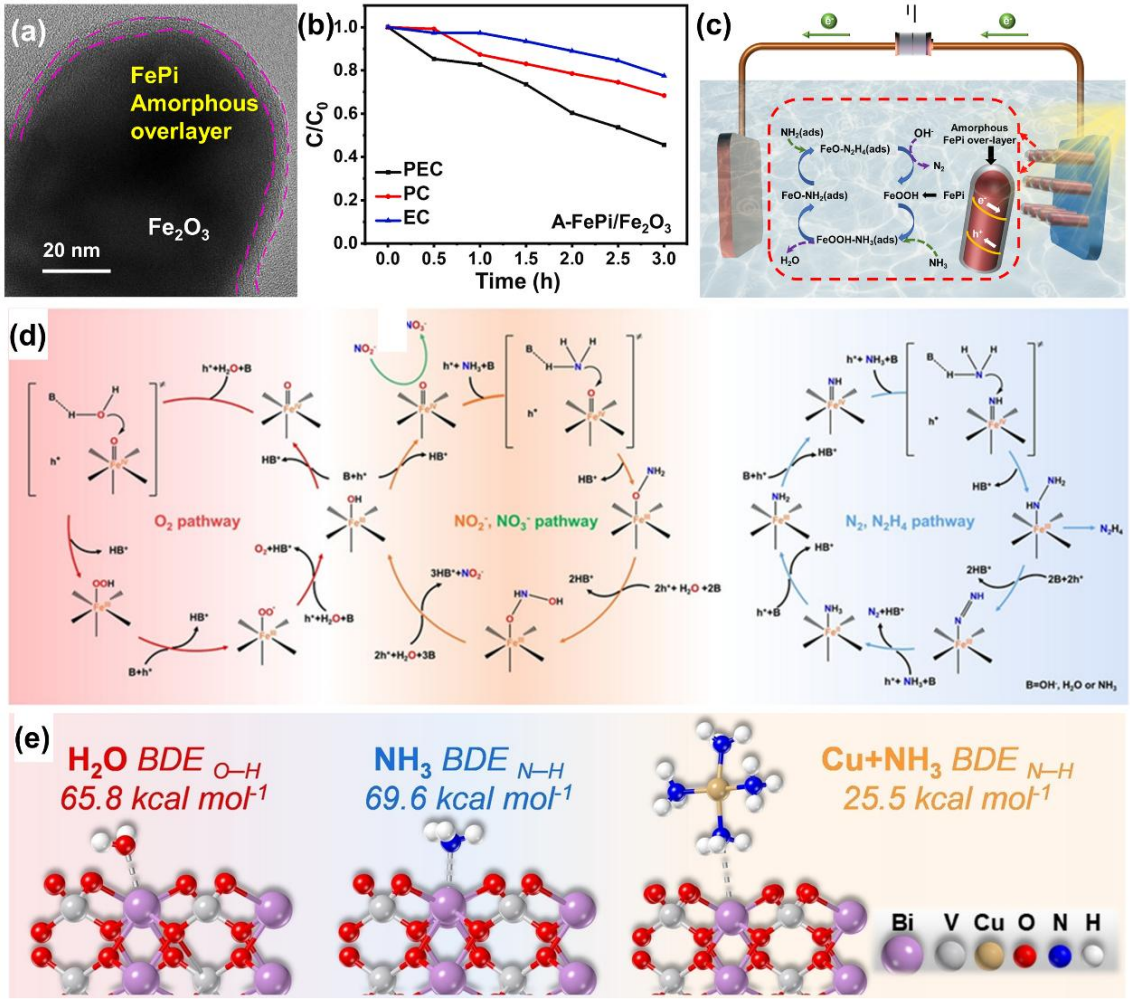

Figure 13. (**a**) Morphology of FePi/Fe_2O_3 photoanode for PEC AOR. (**b**) Ammonia Degradation rate of activated FePi/Fe_2O_3 photoanode in PEC, electrocatalytic and photocatalytic condition. (**c**) Illustration of FePi/Fe_2O_3 photoanode for PEC AOR [129]. Copyright 2020. Elsevier. (**d**) Illustration of α-Fe_2O_3 photoanodes in PEC AOR and the competitive non-radical nucleophilic attack pathways for ammonia oxidation [130]. Copyright 2022. Wiley. (**e**) Comparison of $BDE_{X–H}$ (X=O or N) in three cases on the $BiVO_4$ surface. The dashed bonds represented the adsorption interaction [131]. Copyright 2023.Wiley.

4.3. Alcohols Conversions

The PEC oxidation of alcohols presents a sustainable route for upgrading these platform chemicals into value-added aldehydes, ketones, and carboxylic acids. In PEC alcohols oxidation reaction, the photogenerated holes migrate to the electrode-electrolyte interface, acting as potent oxidants to selectively abstract electrons from adsorbed alcohols molecules [132]. This process is governed by the energy alignment between the semiconductor's valence band and the redox potential of the alcohol/substrate couple [133]. The concurrent application of an external bias enhances charge separation, suppresses electron-hole recombination, and provides independent control over the interfacial potential, enabling precise steering of the reaction pathway toward desired products under mild, often ambient, conditions [134].

Despite this potential, PEC alcohol oxidation faces significant challenges that mirror and extend beyond those of thermal catalytic systems [110]. A primary issue is achieving high selectivity for partial oxidation products—such as converting benzyl alcohol to benzaldehyde or glycerol to dihydroxyacetone—without over-oxidation to carboxylic acids or complete mineralization to CO_2. This selectivity challenge is compounded by the competitive OER, which consumes photogenerated holes and lowers the Faradaic efficiency for the target organic transformation. Furthermore, many robust semiconductor photoanodes possess valence band positions that

thermodynamically favor OER, making kinetic control crucial. Additional hurdles include catalyst deactivation via fouling by organic intermediates, limited light absorption efficiency, and the need for scalable, cost-effective electrode fabrication [135].

To address these challenges, several advanced material and system design strategies have emerged. Band-structure engineering through heterojunction construction like coupling a light-harvesting semiconductor with a catalytic overlayer can create built-in electric fields to improve charge separation while tuning surface energetics for alcohol adsorption over water [22]. The design of tailored active sites can lower the activation barrier for the specific alcohol oxidation step and inhibit OER. Modifying the reaction environment, such as adjusting pH or using alternative redox-mediators, can also shift product selectivity [136]. Recent work further demonstrates the promise of integrating molecular catalysts with semiconductor surfaces to combine the selectivity of homogeneous catalysis with the robustness and light-harvesting properties of solid-state photoelectrodes [137]. By synergistically applying the strategies including optimizing light absorption, charge transport, and surface catalytic kinetics, PEC technology can overcome current limitations and establish itself as a versatile and efficient platform for the sustainable valorization of alcohols.

In this section, the mechanisms of the conversion of various alcohols, including monools, diols, polyols, and more structurally complex aromatic alcohols, into high-value chemical products through photocatalytic alcohol oxidation reactions will be discussed, and strategies for optimizing photoanode materials will be further analyzed in detail.

4.3.1. Vacancy Engineering

Vacancy engineering can be used to effectively modulate the activity and selectivity of (photo)electrocatalysts by artificially introducing defects [138]. For example, in the oxidation reaction of methanol, electron-rich active sites can be formed by creating oxygen holes on the surface of metal oxide catalysts to improve the adsorption and activation of C-H bonds in methanol molecules while promoting photogenerated charge separation to effectively prevent over-oxidation and thus improve the selectivity of the target products [139].

As the simplest saturated monohydric alcohol, the oxidation process of methanol faces several challenges. On the one hand, it is necessary to realize the efficient and selective activation of C-H bonds and to further promote C-C coupling to generate high-value products such as ethylene glycol [140]; on the other hand, it is often difficult to stay in the intermediate stage because the initial oxidation product formaldehyde (HCHO) is more easily oxidized than methanol. The reaction is often difficult to maintain in the intermediate stage and tends to over-oxidize to form CO_2, which leads to a decrease in the selectivity of the target product [141]. Therefore, the targeted conversion of methanol into specific products has become an important scientific topic. Hongwei Huang's team [142] reported for the first time the construction of oxygen vacancies (OVs) on $BiVO_4$ photoanodes by electrolyte photooxidation and revealed the regulatory mechanism of oxygen vacancy-induced catalytic site switching on the selectivity of formaldehyde (HCHO). (Figure 14a) The oxygen hole shifted the adsorption site of CH_3OH from the Bi site to the V site, which enhanced methanol adsorption, lowered the energy barrier of C-H bond activation, and simultaneously promoted the desorption of HCHO, effectively facilitating the separation of photogenerated charge carriers, thus jointly improving the rate and selectivity of formaldehyde production. In a near-neutral electrolyte environment, the BVO-OV photoanode achieved a Faraday efficiency of 94.7% for methanol oxidation at 1.0 V vs. RHE and achieved a high HCHO yield of 579.9 $mmol•m^{-2}•h^{-1}$. This study provides a new idea for the synergistic modulation of vacancies and electrolyte environment to realize high value-added PEC conversions and provides ideal reaction conditions for the conversion of alcohols and aldehydes.

Glycerol is a typical polyol, and it can be used as a raw material to catalytically produce various high-value products such as dihydroxyacetone (DHA), glyceraldehyde, and lactic acid [143]. However, the glycerol molecule contains three hydroxyl groups, which leads to diverse oxidation reaction pathways and complex electron transfer processes, making highly selective value-added conversion difficult to achieve. In glycerol oxidation, these vacancies can effectively modulate the electronic structure of the catalyst and optimize the adsorption behavior of the reaction intermediates, thereby changing the course of the reaction [139,144]. As is shown in Figure 14b, Yuan Lu et al. [145] constructed a $BiVO_{4-x}$ photoanode with bismuth-rich regions synergistically regulated by oxygen vacancies through a combination of hydrothermal seeding method, alkaline etching and electrochemical reduction (Bi-rich $BiVO_{4-x}$). The introduction of oxygen holes not only increases the reaction frequency of the bi-atoms at the interface and the efficiency of charge transfer at the surface, but also acts synergistically with the bismuth-rich surface layer to optimize the adsorption selectivity of glycerol at the electrode surface. Gibbs free energy calculations showed that on the Bi-rich $BiVO_{4-x}$ surface, the free energies of all steps of glycerol sec-hydroxyl oxidation were lower than those of the primary hydroxyl pathway, with a free energy difference of 61.9 kJ/mol

throughout the process, (Figure 14c) which thermodynamically tended to generate DHA significantly, effectively inhibiting C-C bond breaking and over-oxidation of DHA. (Figure 14d) The DHA selectivity of this photoanode was increased to 80.3% with a yield of 361.9 mmol m^{-2} h^{-1} under AM1.5G illumination and 1.23 V vs. RHE. Faraday efficiency analysis showed a significant increase in the contribution of the DHA pathway, while the generation of the primary hydroxyl oxidation products was inhibited. The DHA selectivity was still 70.7% after 5 h of reaction, and the bismuth-rich state and oxygen vacancy structure on the photoanode surface were stable, indicating excellent catalytic durability.

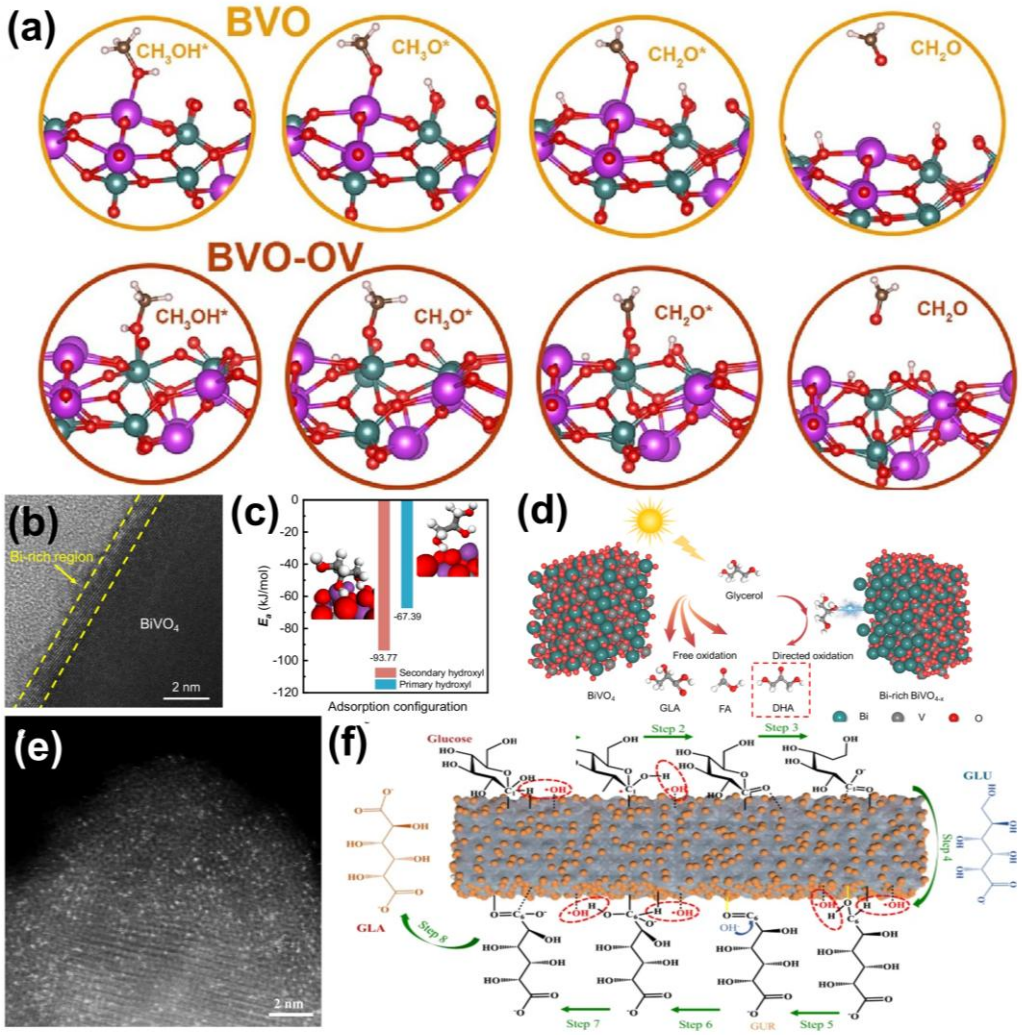

Figure 14. (a) The process of CH3OH oxidation to HCHO for BVO and BVO-OV [142]. Copyright 2023.Elsevier. (**b**) HR-TEM image of Bi-rich $BiVO_{4-x}$. (**c**) The DFT-calculated energies related to glycerol adsorption on the Bi-rich $BiVO_{4-x}$ surface through either the primary or secondary hydroxyl group. (**d**) Schematic illustration of the PEC glycerol oxidation to DHA using Bi-rich $BiVO_{4-x}$ photoanode [145]. Copyright 2024. Springer Nature. (**e**) HAADF-STEM image of Pt/def-TiO_2. (**f**) Schematic illustration of the possible pathway for the PEC oxidation of glucose to GLU and GLA over the Pt/def-TiO_2 photoanode [146]. Copyright 2023. Springer Nature.

Vacancy engineering is a powerful strategy to adjust selectivity for modulating oxidation reactions. By constructing specific vacancies within catalyst materials, it will be able to precisely control the activation of polyhydroxy groups and suppress non-selective over-oxidation pathways. This strategy has also been applied to the value-added conversion of PEC glucose oxidation. Glucose is a typical polyol, also faces the same problem of selective oxidation of polyhydroxyl groups, and its oxidation regulation is even more difficult due to the spatial resistance of the ring structure and the high reactivity of the aldehyde group. Zhangliu Tian et al. [146] constructed monatomic Pt-modified defective TiO_2 (Pt/def-TiO_2) nanorod photoanodes. (Figure 14e) The defective structure (def-TiO_2) was constructed by introducing oxygen vacancies and Ti^{3+}, resulting in the formation of a disordered shell layer that narrows the TiO_2 band gap and expands the light absorption range; at the same time, the top energy

level of the valence band was modulated to prevent C-C bond breakage due to excessive hole energies and to expand the electron conduction range to improve charge separation and transport efficiency. Monoatomic Pt, which uses defect sites to enhance metal-carrier interactions, prevents Pt agglomeration and forms highly active centers. (Figure 14f) The photoanode achieves 98.8% glucose conversion, 84.3% gluconolactone yield and 93.5% overall selectivity for gluconolactone and gluconic acid at 0.6 V vs. RHE. The Faraday efficiency of cathodic hydrogen precipitation was over 99% and the Faraday efficiency of gluconolactone was 86.8%.

In summary, through vacancy engineering, the electronic structure and surface reactivity of the catalyst were successfully modulated by the introduction of defects such as oxygen vacancies, allowing precise control of the reaction pathway in polyol oxidation. Despite the significant progress of this strategy in improving product selectivity and reaction kinetics, the long-term stability of vacancies under reaction conditions is insufficient, and there is still no universal approach for precise modulation of the type, concentration and spatial distribution of vacancies. In the future, we should focus on developing more stable vacancy preparation techniques, combining advanced in situ characterization and theoretical calculations to analyze the regulation mechanism of vacancies on reaction intermediates in depth, and exploring the synergistic effects of vacancies with other modification strategies to extend them to more complex polyol systems.

4.3.2. Co-Catalyst

In alcohols oxidation reaction, co-catalyst do not directly participate in the reaction themselves, but they can significantly improve the selectivity or stability of the reaction [147]. In methanol oxidation reactions, the main role of the co-catalyst is to create an efficient microenvironment for interfacial reactions and accelerate the rate of interfacial charge transfer to the reactants, rather than directly altering the electronic structure of the main catalyst [148].

The modification of co-catalysts is an effective way to optimize the interfacial microenvironment of the methanol oxidation reaction. As is shown in Figure 15a, Sabiha-Sultana et al. [149] constructed an Au-CoO_x core-shell-structured composite co-catalyst for the first time to form a TiO_2-Au-CoO_x composite photoanode, which is an efficient solution to the performance limitations of the TiO_2-based photoanode. This co-catalyst modification strategy breaks the limitation that TiO_2 only absorbs ultraviolet light through the localized surface plasmon resonance effect of Au, which greatly enhances the ability to capture visible light. In addition, Au acts as an electronic bridge to promote an efficient charge transfering from CoO_x to TiO_2, thereby significantly inhibit the photogenerated carrier composition. (Figure 15b) Moreover, the core-shell structure of Au-CoO_x isolated Au from the electrolyte and protected the TiO_2 substrates from being corroded. By rational decorating the cocatalyst, the formaldehyde yield reached 173 μmol/L in the methanol oxidation reaction for 1.5 h under alkaline conditions. Bang-Feng Zheng et al. [150] constructed Au-ZnO/α-Fe_2O_3 core-shell nanotube arrays (NTAs), which enhanced the absorption of visible light by the surface-isolated excitation resonance effect of Au co-catalysts. (Figure 15c) Electrons generated by Au were injected into the conduction band of α- Fe_2O_3, further accelerating the charge separation and charge transfer. The Au-ZnO cocatalyst led to a promoted performance for PEC methanol oxidation reaction with the Faraday efficiency reached as high as 85.5% and good selectivity for formaldehyde.

In the ethylene glycol oxidation reaction, co-catalysts can regulate the electronic structure of the main catalyst, thereby prevent over-oxidation and improve the selectivity of the target product. At the same time, they can provide surface-active oxygen species to accelerate the reaction, thus contributing to efficient conversion. Furthermore, co-catalyst overlayers can prevent photo-corrosion, thereby improving the stability of the photoanode [147,151]. Jingshan Luo's group [152] synthesized a Mo:$BiVO_4$/NiCo-LDH photoanode, (Figure 15d) where NiCo-LDH served as a co-catalyst. The NiCo-LDH cocatalyst effectively protected the $BiVO_4$ substrate, preventing the corrosion of $BiVO_4$ in alkaline conditions. The uniformly loaded NiCo-LDH cocatalyst significantly improved hole extraction capabilities, provided abundant electrochemical oxidation active sites, and suppressed charge recombination and surface defects through the synergistic effect of Ni and Co. The NiCo-LDH cocatalyst overcame the challenges of low charge separation efficiency and slow surface reaction kinetics of pristine $BiVO_4$ in the ethylene glycol oxidation reaction, thus greatly improving the stability and reaction efficiency of the photoanode. This photoanode catalyzed the oxidation of ethylene glycol to formic acid at a potential of 1.0 V vs. RHE, with a Faraday efficiency exceeding 85% and a yield of 1.71 mmol/L.

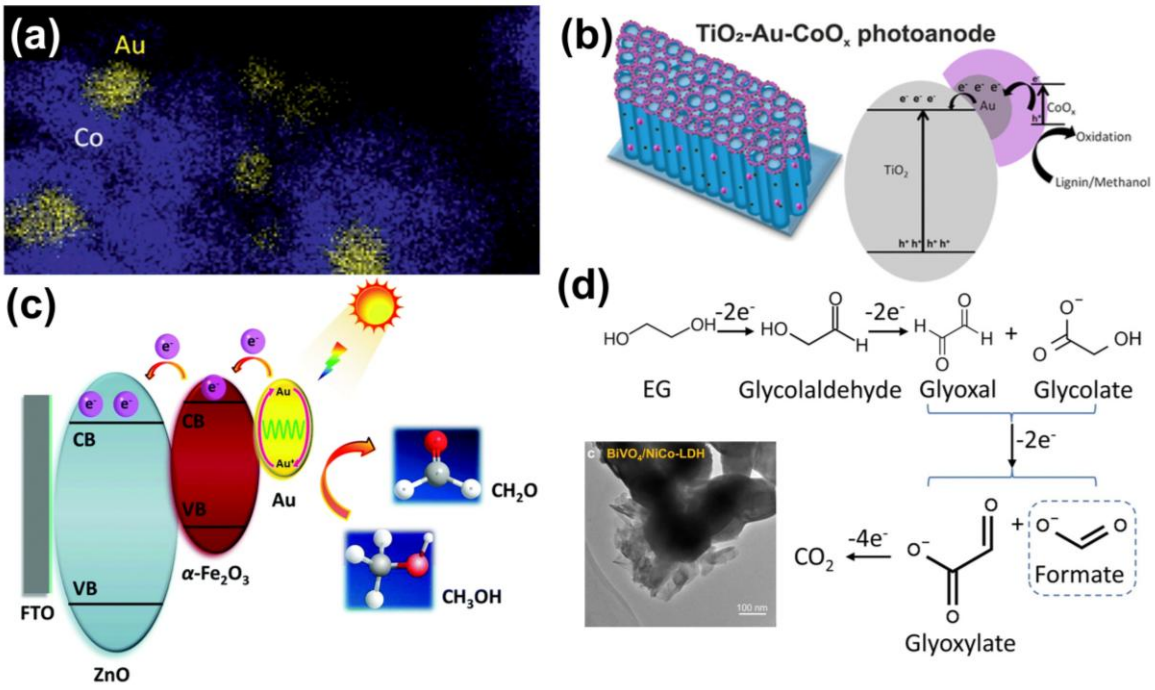

Figure 15. (**a**) EDS scan of TiO_2-Au-CoO_x. (**b**) Schematic illustration of the charge transfer mechanism in TiO_2-Au-CoO_x [149]. Copyright 2024. American Chemical Society. (**c**) Schematic diagram of the proposed MOR mechanism in ZnO/α-Fe_2O_3/Au NTAs hybrid photo-electrocatalysts [150]. Copyright 2018. The Royal Society of Chemistry. (**c**) TEM image of $BiVO_4$/NiCo-LDH photoanode. (**d**) The proposed reaction pathway for the PEC oxidation of EG to formate in alkaline solution [152]. Copyright 2024. Wiley.

4.3.3. Facet Engineering

Facet engineering controls the exposed crystal surfaces of materials, allowing it to preferentially exhibit surface structures with specific atomic arrangements and coordination environments. In the complex reaction of polyol oxidation, different crystal facets exhibit distinctly different adsorption behaviors and activation capabilities for reactant molecules and intermediates due to differences in atomic surface density, geometric configuration, and electronic state distribution. Therefore, crystal facet engineering is widely used in studies aimed at controlling the selectivity of polyol oxidation reactions [153].

In PEC polyol oxidation reaction, by controlling the main facets of photoanode materials, the adsorption and activation pathways of the reactants can be effectively optimized, thereby achieving high selectivity for high-value products and significantly improving the charge separation efficiency. Dong Liu et al. [154] synthesized a $BiVO_4$ photoanode with exposed dominant (112) facets using an electrodeposition method. Glycerol molecules can be efficiently adsorbed on the (112) facets of $BiVO_4$, accelerating the transfer of photogenerated holes to the adsorbed glycerol molecules. (Figure 16a) Therefore, more stable intermediate carbon radicals were generated during the glycerol oxidation process on the $BiVO_4$ surface, effectively improving the product selectivity for DHA production from glycerol oxidation. (Figure 16b) At a voltage of 1.2 V vs. RHE, this photoanode achieved a DHA yield of 200 mmol/(m^2·h), a maximum selectivity of 63.6%, and a Faraday efficiency of approximately 30%. In another research work, Truong-Giang Vo et al. [155] synthesized two kind of $BiVO_4$ with well-defined {010} and {121} crystal orientations. Combining experimental results and DFT stimulations, it demonstrated that the {010} crystal facet was more favorable for glycerol adsorption and photo-induced charge separation compared to the {121} crystal facet, significantly improving reaction efficiency. The yields of DHA and glyceraldehyde from {010}-$BiVO_4$ were more than twice those of samples with a dominant {121}-$BiVO_4$ crystal facet, and the selectivity for the high-value product DHA is approximately 60%. (Figure 16c, d)

In summary, facet engineering can effectively optimize the adsorption and activation pathways of reactants in polyol oxidation reactions, thereby achieving high selectivity for high-value products and significantly improving catalyst separation efficiency. However, precisely controlling interfacial quality remains challenging, and a deeper understanding of the mechanisms between different crystal surfaces and reaction pathways is still needed. Future research should focus on developing simple and practical methods for crystal surface modification

and constructing multi-level crystal surface structures to further promote the practical application of green conversion processes for polyols.

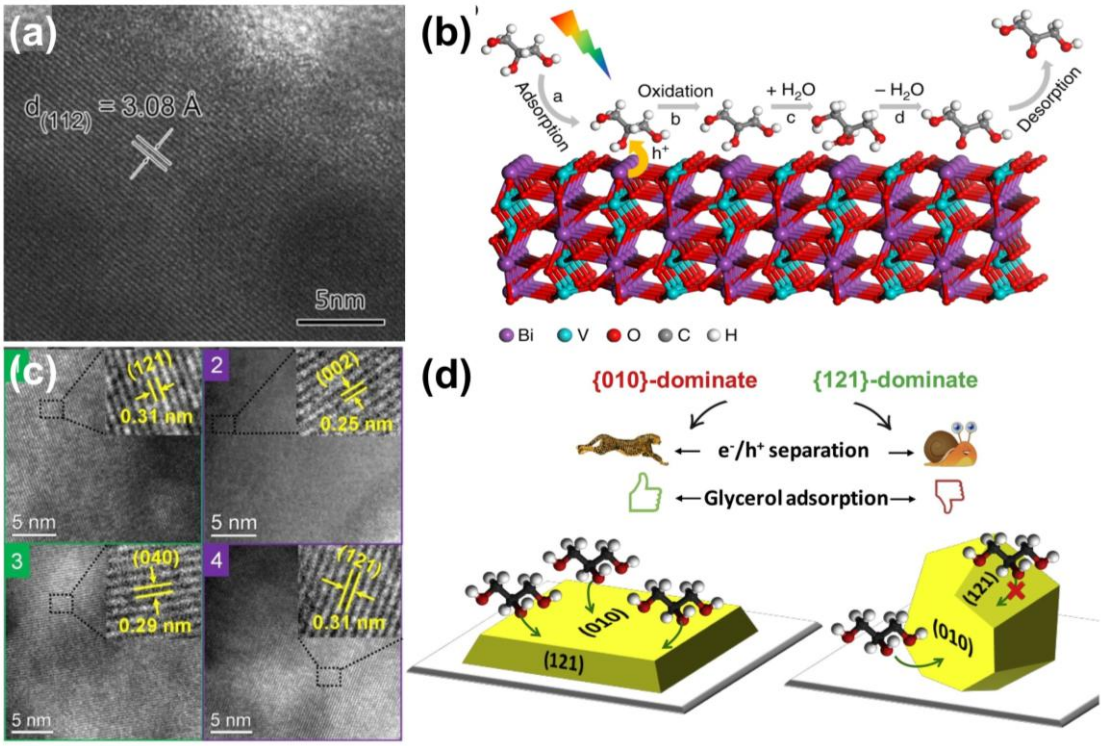

Figure 16. (**a**) HRTEM image of (112)-$BiVO_4$ nanoporous arrays. [154] (**b**) Schematic illustration showing PEC glycerol oxidation to DHA on (112)-$BiVO_4$ [154]. Copyright 2019. Springer Nature. (**c**) HRTEM images of {010}-BVO. (**d**) Illustration of the proposed mechanism for PEC GOR on $BiVO_4$ with different exposed facets [155]. Copyright 2020. Elsevier.

4.3.4. Summary

PEC alcohols oxidation has emerged as a sustainable route for upgrading renewable feedstocks into value-added chemicals. The primary research focus has centered on overcoming the intrinsic selectivity challenges inherent to alcohol oxidation, particularly the competing over-oxidation to carboxylic acids or CO_2, and the kinetically favored but undesired oxygen evolution reaction. Current strategies to enhance selectivity and efficiency are multifaceted, targeting both the catalyst surface and the bulk/interface properties.[156]

A dominant approach involves precise surface engineering to tailor the interaction between the catalyst and alcohol molecules. This includes creating specific defect sites, exposing selective crystal facets, and depositing co-catalysts. These modifications aim to favor the adsorption and activation of the target alcohol's hydroxyl group over water, thereby directing the reaction pathway toward the desired partial oxidation product and suppressing both over-oxidation and oxygen evolution. Concurrently, bulk and interfacial modifications are employed to improve the underlying photoelectrochemical performance. Strategies such as deliberate defect doping and the construction of heterojunctions are implemented to enhance light absorption across a broader spectrum and, more critically, to drastically improve the separation and transport of photogenerated charge carriers. Efficient charge delivery to the surface is a prerequisite for enabling the selective surface reactions to proceed at high rates.

In future, PEC alcohols oxidation will address several interconnected challenges to progress toward practical applications. [157]A key direction is the deeper integration of surface active-site design with bulk/interface charge-management engineering. This requires moving beyond sequential optimization to develop materials where the light-harvesting, charge-separation, and catalytic functions are synergistically designed as a unified system. Furthermore, advancing beyond trial-and-error design necessitates the extensive use of in situ and operando characterization techniques coupled with theoretical modeling. Such efforts are crucial for mapping the dynamic evolution of surface intermediates and active sites under operating conditions, thereby uncovering the definitive structure-selectivity relationships. Ultimately, integrating these advanced catalysts into scalable reactor

architectures that manage mass transport and utilize low-cost, earth-abundant elements will be essential for translating laboratory breakthroughs into viable technologies for the sustainable valorization of alcohol resources.

5. Compared of Nitrogen-Containing Reactions and Alcohol Reactions

In PEC systems, the key distinction between the oxidation of alcohols and that of nitrogen-containing compounds lies in their reaction mechanisms and value-added logic: the oxidation of alcohols follows a radical pathway involving the activation of C-H bonds, focusing on upgrading biomass platform molecules into high-value-added fine chemicals such as aldehydes and acids through precise dehydrogenation processes, thereby achieving a 'waste-to-chemicals' material upgrade; In contrast, the oxidation of nitrogen-containing compounds focuses on the cleavage of N-H or C-N bonds. By exploiting their thermodynamic potential, which is significantly lower than that of the OER, this process not only degrades pollutants but also substantially reduces the energy consumption of the PEC system to promote hydrogen production at the cathode. It can even be coupled with nitrate reduction to synthesize ammonia, achieving a dual environmental and energy synergy of 'pollutant-to-energy'. Therefore, the former utilized photo-generated holes to re-engineer carbon frameworks to enhance material value, whilst the latter leverages the elimination of nitrogen-containing pollutants to drive more efficient energy recovery; together, they expand the boundaries of traditional PEC water splitting, achieving a transition from single oxygen production to the dual production of high-value products.

6. Conclusions and Perspectives

Converting low-value chemical substances such as nitrogen, nitrogen oxides, and alcohols into high-value chemical products through photoelectrochemical reactions is a key frontier in sustainable catalysis, with the potential to integrate hydrogen fuel production and value-added chemical synthesis within a single cycle framework. Photoelectrochemical conversion also offers advantages such as high product selectivity, low energy consumption, and environmental friendliness, providing a promising alternative to traditional thermochemical routes, which often require high temperatures, high pressures, or hazardous reagents. However, despite the surge in research interest in this field in recent years, photoelectrochemical value-added conversion is still limited by slow reaction kinetics, overlapping reduction pathways, and limited selectivity towards target organic nitrogen products. Substantial progress requires not only the design of more active and selective catalysts but also a comprehensive understanding of reaction mechanisms, interfacial charge dynamics, and reactor designing [158]. Substantial progress requires not only the design of more active and selective catalysts but also a comprehensive understanding of reaction mechanisms, interfacial charge dynamics, and reactor-level phenomena. This chapter will highlight the major scientific challenges and propose forward-looking strategies to guide the next generation of research in this emerging field.

6.1. Quantitative Detection and Mechanistic Visualization

Photoelectrochemical valorization reactions face a fundamental challenge due to the complexity of their intermediate products and the multiplicity of potential reaction pathways, complicating the precise identification of target species. Furthermore, alcohols oxidation reactions can simultaneously produce multiple structurally similar isomers, making precise identification of product components difficult. Therefore, clear elucidations of the specific products and transient intermediates is therefore essential for mechanistic understanding. In situ and operando spectroscopic techniques, such as infrared (IR), Raman, ultraviolet–visible (UV–Vis), and X-ray absorption (XAS) spectroscopy, enable the real-time monitoring of adsorbed intermediates and the dynamic evolution of active sites. These methods are instrumental in detecting transient species like *COOH, *CO, *NO, and *NH_2, thereby providing key evidence for the complex transformation processes of nitrogen-containing compounds and organic molecules. However, each analytical technique possesses inherent limitations. For instance, UV-Vis spectra are often complicated by signal overlap and fluorescence backgrounds, while Raman and IR spectroscopy may suffer from weak signal intensities in aqueous media. To obtain more reliable mechanistic information, a multimodal characterization approach is essential. Combining techniques such as surface-enhanced Raman scattering (SERS), synchrotron-based XAS, and differential electrochemical mass spectrometry (DEMS) can yield complementary insights into electronic structure, molecular composition, and reaction kinetics. This comprehensive operando analytical framework is crucial for unraveling catalytic cycles and identifying the microscopic factors that govern bond-forming events in complex photoelectrochemical transformations.

6.2. Rational Kinetics Optimization

Taking the glucose oxidation reaction as an example, from the perspective of chemical reaction principles, the low selectivity of polyol oxidation reactions is mainly related to the following factors. Firstly, the glucose molecule (participating in the reaction in its chain structure) simultaneously possesses an aldehyde group (-CHO), a primary hydroxyl group (-CH_2OH), and multiple secondary hydroxyl groups (-CHOH). The oxidation potentials of these functional groups are similar, leading to competition for active sites at the electrocatalytic interface and parallel reactions. Even small differences in the initial attack site can lead to completely different products. Secondly, the target product such as glucaric acid is usually an unstable intermediate, which is easily further oxidized on the electrode surface under actual reaction conditions, leading to C-C bond cleavage and the formation of smaller molecules such as oxalic acid and formic acid, or even complete oxidation to CO_2. Simultaneously, this is a typical thermodynamically spontaneous process, making it difficult to completely prevent it. Therefore, the key to highly selective production of specific products in photoelectrochemical upgrading transformations lies in the precise control of the adsorption and desorption of substances on the catalyst surface. A delicate balance between adsorption strength and surface mobility determines whether intermediates undergo coupling, desorption, or competitive side reactions. Designing catalysts with diatomic or heteroatomic active sites offers a promising approach to achieving this goal. For example, Cu-Co bridge sites promote the dehydrogenation of hydroxyl groups, Cu-Cu bridge sites promote the dehydrogenation of carbon to form aldehyde groups, while Cu-Ni bridge sites can promote the oxidation of aldehyde groups to carboxyl groups. Through multi-site synergistic catalysis using high-entropy hydroxides, a glucaric acid yield exceeding 90% has been achieved [159]. Electronic structure tuning through heterostructure or vacancy engineering can further optimize the band center and fine-tune the adsorption energy, making the target reaction more favorable than the oxygen evolution reaction or hydrogen evolution reaction. Furthermore, environmental factors, including electrolyte composition, pH, and local electric field, also play a significant role in PEC valorization. For instance, alkaline electrolytes can suppress proton activity and mitigate the hydrogen evolution reaction, while buffer solutions containing nitrates or nitrites can facilitate nitrogen activation. Future research should combine theoretical screening with microkinetic modeling to establish quantitative correlations between electronic structure, adsorption energy, and overall selectivity. Through these efforts, rational control of intermediate binding can evolve from empirical adjustment to predictive design.

6.3. Rational Thermodynamics Designing

The PEC valorizations of cathodic and anodic reactions inherently compete with various side reactions, the most prominent of which include the HER, OER, carbon dioxide reduction to hydrocarbons, and independent nitrogen oxide reduction pathways [19]. These parallel reactions not only reduce the utilization efficiency of carbon and nitrogen but also complicate mechanistic analysis. To minimize this competition, spatial and electronic separation of active sites has proven to be an effective strategy. Bifunctional catalysts capable of separating the carbon dioxide and nitrogen oxide reduction regions can preferentially direct electron flow towards coupled intermediates. Similarly, surface charge engineering, such as doping, interfacial polarization, or external electric fields, can alter the local potential distribution, thereby suppressing unwanted reactions. Adjusting the electrolyte type, pH, and applied potential remains an effective but underutilized means of controlling reaction selectivity. Looking ahead, combining computationally derived potential-dependent energy diagrams with experimental in-situ spectroscopy holds promise for achieving dynamic control of the reaction environment. Ultimately, achieving near-complete target product production requires not only highly efficient catalysts but also ingenious reaction control strategies to coordinate charge transfer, mass transport, and interfacial energetics.

6.4. Reactor and System Designing

While catalyst development is core issue of advancing PEC valorizations, progress at the reactor and system level is equally critical for transitioning laboratory discoveries toward scalable implementation [160]. Though conventional H-cell configurations is useful for fundamental studies, it usually suffers from mass-transport limitations and inefficient product management. In contrast, flow-cell and gas-diffusion electrode designs enable sustained reactant delivery and can support current densities exceeding 100 mA cm^{-2}, enhancing their suitability for larger-scale operation. The engineering of electrode–electrolyte interfaces—through approaches such as hydrophobic modification, tailored porosity, or advanced electrode fabrication—can improve local reaction environments and mitigate issues like flooding under high-current conditions. Furthermore, integrating photoelectrochemical systems directly with renewable electricity sources, such as photovoltaics or wind power, strengthens the overall sustainability profile of the technology. Realizing these system-level advances requires collaborative efforts across electrochemistry, materials science, and process engineering to establish reliable

performance benchmarks—including Faradaic efficiency, energy conversion efficiency, and operational stability—under conditions relevant to practical application.

In summary, PEC valorizations have transitioned from a conceptual proposition to an active area of investigation that merges sustainable energy conversion with the synthesis of value-added chemicals. Its further advancement necessitates a holistic integration of diverse disciplines, spanning from atomic-scale mechanistic insights to reactor engineering and comprehensive system-level sustainability assessment. Future breakthroughs are anticipated to arise from the synergistic optimization of catalyst architectures, in-situ diagnostics, and process intensification, all guided by the overarching principles of selectivity, scalability, and resource circularity. As these multidimensional efforts converge, photoelectrochemical upgrading is poised to redefine synthetic methodologies for organic compounds and to broadly influence electrochemical manufacturing, thereby supporting a more sustainable chemical industry with harmonized carbon and nitrogen cycles.

6.5. Research Areas at PEC and Interdisciplinary Studies

The current research on PEC valorizations is primarily characterized by the rational design of high-efficiency photoelectrode materials and the diversification of reaction pathways. Researchers are continuously striving to overcome bottlenecks in charge recombination and surface reaction kinetics through the precise control of semiconductor band structures, nanoscale morphology and co-catalysts. Therefore, PEC research is shifting from traditional water splitting for hydrogen production towards the synthesis of high-value chemicals with greater economic potential. On the one hand, thermodynamically more favorable reactions such as UOR or AOR are being utilized to replace the slow oxygen evolution reaction, thereby reducing the energy consumption of hydrogen production whilst treating nitrogen-containing pollutants; on the other hand, the focus is on value-added oxidation of biomass alcohols at the photoanode, as well as driving CO2 reduction or NRR at the photoanode, with the aim of achieving artificial photosynthesis under mild conditions to convert solar energy into hydrocarbon fuels or ammonia.[161]

Secondly, cutting-edge research in this field is accelerating towards the engineering of emerging interdisciplinary technologies and devices. For example, bio-photoelectrochemical cells (BPECs) integrate semiconductors with microorganisms or enzymes, utilising the selectivity and self-repairing capabilities of biological processes to open up new pathways for sustainable energy and environmental remediation; Meanwhile, perovskite materials with excellent optoelectronic properties are being widely applied in research into high-efficiency PEC devices and photovoltaic-electrochemical (PV-EC) tandem devices. More importantly, the focus of research is shifting from material optimization at the laboratory scale to the large-scale fabrication and commercial validation of large-area devices, with a particular emphasis on system integration, long-term operational stability and machine learning-assisted material screening, aiming ultimately to achieve an efficient, stable and economically viable conversion of solar energy into chemical energy.

6.6. Recent Advances in Photocatalysis Research

In recent years, research into photocatalytic materials has primarily focused on two main areas: the oxidation of organic compounds at the anode and the reduction of nitrogen at the cathode. Anode materials, such as BiVO4, Fe2O3 and TiO2-based composites, have demonstrated exceptional selectivity and Faradaic efficiency in the oxidation of substrates such as methanol and glycerol to produce high-value-added chemicals. Cathode materials, meanwhile, have focused on silicon-based, metal/semiconductor composite and two-dimensional materials for the reduction of nitrate ions or nitrogen gas to ammonia. Although selectivity and yield vary considerably, the Faradaic efficiency in certain systems, such as O2SiNW/Au and p-type silicon, has exceeded 95%. Overall, enhancing catalytic performance and product selectivity through the construction of heterostructures, defect engineering and nanostructure regulation represents the core trend in current research (Tables 1 and 2).

Table 1. Summary of recent progress on PEC alcohols oxidation researches.

Photoanode	Electrolyte	Dominant Product	Selectivity [%]	Production [mmol m^{-2} h^{-1}]	FE [%]	Refs.
BVO-OV2	0.1M Na_2SO_4 + 1M CH_3OH	HCHO	94.7	579.9	94.7	[142]
V_0-α-Fe_2O_3PNRs/Pt_{ED}	1 M KOH + 1 M CH_3OH	HCHO	95	-	95	[162]
TiO_2-Au-CoO_x	0.1 M KNO_3 + 0.1 M KOH + 95 vol% CH_3OH	HCHO	＞80	115	≈30–40	[149]
α-Fe_2O_3/$CoFe_2O_4$	-	HCHO	≈97.8	-	97.8	[163]
BG-m-ZrO_2	1 M KOH + 1 M C_2H_5OH	CH_3COOH	≈100	-	-	[164]
ZnO/α- Fe_2O_3/Au NTAs	95 vol% Methanol + 0.1 M NaOH	HCHO	-	-	85.5	[150]
Fe_2O_3/MoO_3	1 M KOH + 1 M CH_3OH	HCHO	≈95.7	-	95.7	[165]
$BiVO_4$/NiCo-LDH	0.1M KOH+10 mM glucose	HCOOH	> 85%	-	85	[152]
PdAgCu NSs/GCE	1 M KOH + 1 M EG	HCOOH	≈90	-	≈90	[166]
Au_1Ag_1 nanobowls/GCE	1 M KOH + 1 M EG	$C_2O_4^{2-}$	95	345	90–95	[167]
$BiVO_4$ nanoarrays	0.5 M Na_2SO_4 + 0.1M glycerol	DHA	51	200	30	[154]
Bi-rich $BiVO_{4-x}$	0.5 M Na_2SO_4 + 0.1 M glycerol	DHA	80.3	361.9	-	[145]
m-H-WO_3/TiO_2	0.5 M Na_2SO_4 + 0.1 M glycerol + 0.1 M boric acid buffer	GLAD、DHA	85	353	70	[168]
Pt/def-TiO_2 NRAs	1 M KOH + 10 mM glucose	GLA	85.3	307	86.8	[146]
002-$W0_3$	0.5 M H_2SO_4 + 0.1 M glycerol	GLYA	73	32.3	39	[169]
{010}-BVO	0.1 M $Na_2B_4O_7$ + 0.1 M glycerol	DHA	60	-	92	[154]
Bi_2MoO_6@TiO_2 NTA	0.1 M Na_2SO_4 + 0.1 M BA	BAD	98.6	-	98.6	[170]
TiO_2/Fe_2O_3	90% MeCN + 10% H_2O, 0.1 M $TBABF_4$, 20 mM PA, 40 mM TEMPO	piperonal	100	312	＞95	[171]
$BiVO_4$/U-LDH/G	0.1 M PBS+ 0.2 M BA	BAD	＞99	≈867	≈97	[172]

Table 2. Summary of recent progress on photocathodes for PEC valorizations.

Photoanode	Electrolyte	Dominant Product	Selectivity [%]	Production [mmol m^{-2} h^{-1}]	FE [%]	Refs.
p-type Si	0.2 M LiBF4 1.0 vol % EtOH	NH_3	95%	30.80	95.00	[70]
Si/Cu-NSTL/$Co(OH)_2$	0.1 M KOH 0.1 M KNO_3	NH_3	~100%	223.00–1066.00	≈100.00	[87]
Ni/c-Si ABC	1 M KOH 0.5 M KNO_3	NH_3	-	1449.00	85.00	[75]
Au grating/TiB2@AuNPs	0.1 M Na_2SO_4	NH_3	>61.8%	1.88	31.70	[47]
n^+np^+-Si	0.05 M H_2SO_4 Ar N_2	NH_3	-	0.08	61.80	[65]
O_SiNW/Au	0.5 M K_2SO_4 Ar 10 mM KNO_3	NH_3	95.6%	—	95.60	[80]
BP NS/ITO-LbL	0.1 M HCl N_2	NH_3	-	6.02	23.30	[46]
V_o-SnO_2/TiO_2	0.1 M Na_2SO_4 N_2	NH_3	-	1.14	59.60	[51]
NV-g-C_3N_5/BiOBr	0.05 M HCl 0.05 M Na_2SO_4	NH_3	>61.8%	17.3	11.00	[50]
Ti–WO_3/$SrWO_4$	Ar N_2	NH_3	-	6.57	13.42	[67]
Mo_2C/GaN/InGaN	0.05 M H_2SO_4	NH_3	-	4.66	15.39	[66]
Cu/C/Si	1 M KOH 50 mM KNO_3	NH_3	88%	1153.00	88.00	[86]

6.7. Developments in Optoelectronic Devices

The development of PEC devices is undergoing a profound shift from the optimization of individual materials towards system integration and engineering applications. At the material level, research focus has shifted from traditional wide-bandgap metal oxides to multi-material systems. Silicon-based photoelectrodes, in particular, are regarded as ideal candidates for industrialization due to their mature fabrication processes and suitable bandgap. Meanwhile, emerging photoactive materials such as perovskites, metal chalcogenides and MOF-based composites are continually emerging, offering a wealth of options for breakthroughs in device performance. At the device architecture level, tandem PEC cells achieve segmented utilization of the solar spectrum through the monolithic integration of wide-bandgap photoanodes with narrow-bandgap photocathodes, with STH efficiency having exceeded 10%. Meanwhile, self-powered dual-photoelectrode systems use the Fermi level difference between the photoanode and photocathode to drive reactions without the need for an external bias, demonstrating unique advantages in sensing and low-energy-consumption hydrogen production. In terms of application expansion, PEC devices have evolved from traditional water splitting for hydrogen production to encompass CO_2 reduction for carbon-based fuel production, the conversion of nitrogen-containing pollutants, value-added oxidation of biomass, and self-powered photoelectric detection, amongst other directions. Currently, device development is facing a critical transition from small-scale laboratory-scale fabrication to large-area mass production. Researchers are advancing PEC devices towards high-efficiency, stable and low-cost practical applications through strategies such as operating under pressure to suppress bubble loss, developing protective layers to enhance stability, and exploring continuous-flow reactors to optimize mass transfer.

Author Contributions

J.J., H.W.: data curation, writing—original draft preparation; Q.L.: conceptualization, methodology, data curation; J.W., Y.Y.: visualization; Y.L.: conceptualization, methodology; C.X.: supervision, writing—reviewing and editing, funding. All authors have read and agreed to the published version of the manuscript.

Funding

This work was supported by the National Natural Science Foundation of China (No. 52402320), Fundamental Research Program of Shanxi Province (No. 202403021212125), and the Postdoctoral Fellowship Program of CPSF under Grant Number GZC20241572. Research Project Supported by Shanxi Scholarship Council of China (2025-042).

Institutional Review Board Statement

Not applicable.

Informed Consent Statement

Not applicable.

Data Availability Statement

We declare that we have no financial and personal relationship with other people or organizations that can inappropriately influence our work, and there is no professional or other personal interest of any nature or kind in any data, service, product and/or company that could be construed as influencing the position presented in the manuscript entitled.

Conflicts of Interest

The authors declare no conflict of interest.

Use of AI and AI-assisted Technologies

No AI tools were utilized for this paper.

References

1. Achakulwisut, P.; Erickson, P.; Guivarch, C.; et al. Global fossil fuel reduction pathways under different climate mitigation strategies and ambitions. *Nat. Commun.* **2023**, *14*, 5425.

2. Cui, J.; Deng, O.; Zheng, M.; et al. Warming exacerbates global inequality in forest carbon and nitrogen cycles. *Nat. Commun.* **2024**, *15*, 9185.
3. Mokaya, M.; Imrie, F.; van Hoorn, W.P.; et al. Testing the limits of SMILES-based de novo molecular generation with curriculum and deep reinforcement learning. *Nat. Mach. Intell.* **2023**, *5*, 386–394. https://doi.org/10.1038/s42256-023-00636-2.
4. Bongaarts, J. IPCC, 2023: Climate Change 2023: Synthesis Report: A Report of the Intergovernmental Panel on Climate Change. *Popul. Dev. Rev.* **2024**, *50*, 577–580. https://doi.org/10.1111/padr.12632.
5. Chen, S.; Chang, X.; Sun, G.; et al. Propane dehydrogenation: Catalyst development, new chemistry, and emerging technologies. *Chem. Soc. Rev.* **2021**, *50*, 3315–3354. https://doi.org/10.1039/d0cs00814a.
6. Fujishima, A.; Honda, K. Electrochemical Photolysis of Water at a Semiconductor Electrode. *Nature* **1972**, *238*, 37–38. https://doi.org/10.1038/238037a0.
7. Li, W.; Wang, D.; Zhang, Y.; et al. Defect Engineering for Fuel-Cell Electrocatalysts. *Adv. Mater.* **2020**, *32*, 1907879. https://doi.org/10.1002/adma.201907879.
8. Biju, A.T.; Kuhl, N.; Glorius, F. Extending NHC-Catalysis: Coupling Aldehydes with Unconventional Reaction Partners. *Acc. Chem. Res.* **2011**, *44*, 1182–1195. https://doi.org/10.1021/ar2000716.
9. Yan, Y.; Zhou, H.; Xu, S.-M.; et al. Electrocatalytic Upcycling of Biomass and Plastic Wastes to Biodegradable Polymer Monomers and Hydrogen Fuel at High Current Densities. *J. Am. Chem. Soc.* **2023**, *145*, 6144–6155. https://doi.org/10.1021/jacs.2c11861.
10. Zhang, Y.; Li, G.; Wang, L.; et al. Fusion of Multi-Resonance Fragment with Conventional Polycyclic Aromatic Hydrocarbon for Nearly BT.2020 Green Emission. *Angew. Chem. Int. Ed.* **2022**, *61*, e202202380. https://doi.org/10.1002/anie.202202380.
11. Li, E.; Liu, C.; Lin, H.; et al. Bonding Strength Regulates Anchoring-Based Self-Assembly Monolayers for Efficient and Stable Perovskite Solar Cells. *Adv. Funct. Mater.* **2021**, *31*, 2103847. https://doi.org/10.1002/adfm.202103847.
12. Fang, W.; Liu, S.; Steffensen, A.K.; et al. On the Role of Cu+ and CuNi Alloy Phases in Mesoporous CuNi Catalyst for Furfural Hydrogenation. *ACS Catal.* **2023**, *13*, 8437–8444. https://doi.org/10.1021/acscatal.3c01767.
13. Lin, S.; Zhang, H.; Wang, C.; et al. Metabolomics Reveal Nanoplastic-Induced Mitochondrial Damage in Human Liver and Lung Cells. *Environ. Sci. Technol.* **2022**, *56*, 12483–12493. https://doi.org/10.1021/acs.est.2c03980.
14. Berger, M.; Ma, D.; Baumgartner, Y.; et al. Stereoselective conjugate cyanation of enals by combining photoredox and organocatalysis. *Nat. Catal.* **2023**, *6*, 332–338. https://doi.org/10.1038/s41929-023-00939-y.
15. Pan, J.; Li, M.; Wang, Y.; et al. Advanced photoelectrocatalytic coupling reactions. *Chin. J. Catal.* **2025**, *73*, 99–145. https://doi.org/10.1016/s1872-2067(25)64697-3.
16. Jing, L.; Xu, Y.; Xie, M.; et al. Piezo-photocatalysts in the field of energy and environment: Designs, applications, and prospects. *Nano Energy* **2023**, *112*, 108508. https://doi.org/10.1016/j.nanoen.2023.108508.
17. Knöppel, J.; Kormányos, A.; Mayerhöfer, B.; et al. Dissolution Stability of Photoanodes and Co-Catalysts in Photoelectrochemical Water Splitting. *ECS Meet. Abstr.* **2020**, *45*, 2550–2550. https://doi.org/10.1149/ma2020-01452550mtgabs.
18. Kang, S.H. Utilizing a High-Efficiency and Durable Electrocatalyst on GaAs for PEC Water Oxidation. *ECS Meet. Abstr.* **2024**, *59*, 4020–4020. https://doi.org/10.1149/ma2024-02594020mtgabs.
19. Zuo, L.; Deng, Y.; Chen, L.; et al. Fundamental insights into photoelectrochemical carbon dioxide reduction: Elucidating the reaction pathways. *ACS Catal.* **2024**, *14*, 16795–16833.
20. Zhao, Z.; Murad, M.; Pei, C.; et al. Rational Design of Heterostructured MXene-Based Nanomaterials in Electrocatalytic Water Splitting. *ChemCatChem* **2025**, *17*, e202401261. https://doi.org/10.1002/cctc.202401261.
21. Durante, C.; Mazzucato, M.; Bellardita, M.; et al. Fundamentals of photoelectrocatalysis. *Photoelectrocatalysis* **2023**, 7-81. https://doi.org/10.1016/b978-0-12-823989-6.00003-5.
22. Zhang, J.; Wang, X.; Wang, X.; et al. Heterophase junction effect on photogenerated charge separation in photocatalysis and photoelectrocatalysis. *Acc. Chem. Res.* **2025**, *58*, 787–798.
23. Thomas, K.G.; Kamat, P.V. Chromophore-Functionalized Gold Nanoparticles. *Acc. Chem. Res.* **2003**, *36*, 888–898. https://doi.org/10.1021/ar030030h.
24. Li, P.; Liu, Y.; Shi, S.; et al. Highly Crystalline Graphene Fibers with Superior Strength and Conductivities by Plasticization Spinning. *Adv. Funct. Mater.* **2020**, *30*, 2006584. https://doi.org/10.1002/adfm.202006584.
25. Olean-Oliveira, A.; Hasnain, N.; Čolić, V. Determining the Faradaic Efficiency and Selectivity Using a Rotating Ring-Disk Electrode at Low and Intermediate Rotation Rates: Example of the Oxygen Reduction Reaction on Carbon Materials. *ACS Electrochem.* **2025**, *1*, 1878–1883. https://doi.org/10.1021/acselectrochem.5c00295.
26. Zhao, Z.; Deng, H.; Wang, W.; et al. Faradaic Efficiency Acquisition Along with Hydrogen Generation Measurement of Proton Conducting Solid Oxide Electrolysis Cells: Insights from Idaho National Laboratory. *ECS Meet. Abstr.* **2024**, *48*, 3329–3329. https://doi.org/10.1149/ma2024-02483329mtgabs.

27. Cao, X.; Wulan, B.; Wang, Y.; et al. Atomic bismuth induced ensemble sites with indium towards highly efficient and stable electrocatalytic reduction of carbon dioxide. *Sci. Bull.* **2023**, *68*, 1008–1016. https://doi.org/10.1016/j.scib.2023.04.026.
28. Shi, R.; Zhang, X.; Waterhouse, G.I.N.; et al. The Journey toward Low Temperature, Low Pressure Catalytic Nitrogen Fixation. *Adv. Energy Mater.* **2020**, *10*, 2000659. https://doi.org/10.1002/aenm.202000659.
29. Zeng, X.; Zhang, S.; Liu, Y.; et al. Energy-Efficient Pathways for Pulsed-Plasma-Activated Sustainable Ammonia Synthesis. *ACS Sustain. Chem. Amp; Eng.* **2023**, *11*, 1110–1120. https://doi.org/10.1021/acssuschemeng.2c06259.
30. de la Hera, G.; Ruiz-Gutiérrez, G.; Viguri, J.R.; et al. Flexible Green Ammonia Production Plants: Small-Scale Simulations Based on Energy Aspects. *Environments* **2024**, *11*, 71. https://doi.org/10.3390/environments11040071.
31. Li, Y.; Li, S.; Huang, H. Defective photocathode: Fundamentals, construction, and catalytic energy conversion. *Adv. Funct. Mater.* **2023**, *33*, 2304925.
32. Khan, A.; Abbas, A.; Dickson, R. Towards a low-carbon future: Exploring green urea synthesis for sustainable agriculture. *Green. Chem.* **2024**, *26*, 1551–1565. https://doi.org/10.1039/d3gc03228k.
33. Ying, Y.; Fan, K.; Qiao, J.; et al. Rational Design of Atomic Site Catalysts for Electrocatalytic Nitrogen Reduction Reaction: One Step Closer to Optimum Activity and Selectivity. *Electrochem. Energy Rev.* **2022**, *5*, 6. https://doi.org/10.1007/s41918-022-00164-4.
34. Shetty, A.U.; Sankannavar, R. Exploring nitrogen reduction reaction mechanisms in electrocatalytic ammonia synthesis: A comprehensive review. *J. Energy Chem.* **2024**, *92*, 681–697. https://doi.org/10.1016/j.jechem.2024.01.024.
35. Guo, W.; Zhang, K.; Liang, Z.; et al. Electrochemical nitrogen fixation and utilization: Theories, advanced catalyst materials and system design. *Chem. Soc. Rev.* **2019**, *48*, 5658–5716.
36. Teja, D.S.; Mallik, B.S. Breaking the Barrier: How Alkali Cations Promote Enhanced N₂ Adsorption and *NNH Formation. *ACS Catal.* **2025**, *15*, 15287–15301. https://doi.org/10.1021/acscatal.5c04857.
37. Stem, D.; Akter, T.; Barile, C.J. Improving the Catalytic Efficiency of Electrochemical Nitrogen Reduction Reaction (NRR) through Surface Modification and Nanostructured Bimetallic Catalysts. *ECS Meet. Abstr.* **2024**, *39*, 2307–2307. https://doi.org/10.1149/ma2024-01392307mtgabs.
38. Ali, K.; Lu, Y.; Murad, M.; et al. Dimension-dependent heterostructure catalysts for acidic oxygen evolution reaction: Challenges and prospects. *Coord. Chem. Rev.* **2026**, *547*, 217072. https://doi.org/10.1016/j.ccr.2025.217072.
39. Zhang, Z.; Ma, W.; Qiao, J.; et al. Exploring dual-iron atomic catalysts for efficient nitrogen reduction: A comprehensive study on structural and electronic optimization. *Nanoscale* **2025**, *17*, 13939–13950. https://doi.org/10.1039/d5nr00426h.
40. Zheng, Y.; Yang, J.; Liu, Z.; et al. Multi-Component Crystalline Mesoporous Materials: Synthesis Principle and Application. *Adv. Mater.* **2025**, *37*, e10911.
41. Chen, X.; Su, H.; Li, T.; et al. Structural and Interfacial Design of Atomically Thin Materials and Their Heterostructures for Advancing Electrocatalysis. *Adv. Mater.* **2025**, *38*, e15722.
42. Ye, Z.; Chen, C.; Su, Y.; et al. Templating Methods for Materials Fabrication Across Scales. *Chem. Rev.* **2025**, *126*, 717–798.
43. Ren, F.; Han, Z.; Zhu, L.; et al. Metallene: Ångström-Scale 2D Metals. *Adv. Mater.* **2026**, *38*, e12683.
44. Li, X.; Guan, X.; Zhu, L.; et al. Electron transfer in catalysis: From fundamentals to strategies. *Chem. Soc. Rev.* **2025**, *54*, 11423–11467.
45. Wu, M.; Dong, F.; Yang, Y.; et al. Emerging Atomically Precise Metal Nanoclusters and Ultrasmall Nanoparticles for Efficient Electrochemical Energy Catalysis: Synthesis Strategies and Surface/Interface Engineering. *Electrochem. Energy Rev.* **2024**, *7*, 10. https://doi.org/10.1007/s41918-024-00217-w.
46. Liu, D.; Wang, J.; Bian, S.; et al. Photoelectrochemical Synthesis of Ammonia with Black Phosphorus. *Adv. Funct. Mater.* **2020**, *30*, 2002731. https://doi.org/10.1002/adfm.202002731.
47. Zabelina, A.; Miliutina, E.; Dedek, J.; et al. Nitrogen Photoelectrochemical Reduction on TiB2 Surface Plasmon Coupling Allows Us to Reach Enhanced Efficiency of Ammonia Production. *ACS Catal.* **2023**, *13*, 10916–10926. https://doi.org/10.1021/acscatal.3c03210.
48. Ali, H.; Ajmal, Z.; Alzahrani, A.Y.A.; et al. Defect-driven innovations in photocatalysts: Pathways to enhanced photocatalytic applications. *InfoMat* **2025**, *7*, e70040.
49. Guo, D.; Wang, S.; Xu, J.; et al. Defect and interface engineering for electrochemical nitrogen reduction reaction under ambient conditions. *J. Energy Chem.* **2022**, *65*, 448–468. https://doi.org/10.1016/j.jechem.2021.06.012.
50. Li, M.; Lu, Q.; Liu, M.; et al. Photoinduced Charge Separation via the Double-Electron Transfer Mechanism in Nitrogen Vacancies g-C(3)N(5)/BiOBr for the Photoelectrochemical Nitrogen Reduction. *ACS Appl. Mater. Interfaces* **2020**, *12*, 38266–38274. https://doi.org/10.1021/acsami.0c11894.
51. Ma, J.; Fu, J.; Sun, L.; et al. Photoelectrochemical-driven nitrogen reduction to ammonia by a V(o)-SnO(2)/TiO(2) composite electrode. *Nanoscale* **2024**, *16*, 5706–5714. https://doi.org/10.1039/d4nr00060a.
52. Pan, Z.; Han, E.; Zheng, J.; et al. Highly Efficient Photoelectrocatalytic Reduction of CO2 to Methanol by a p–n Heterojunction CeO2/CuO/Cu Catalyst. *Nano-Micro Lett.* **2020**, *12*, 18. https://doi.org/10.1007/s40820-019-0354-1.

53. Wang, K.; Yang, Y.; Farhan, S.; et al. S-scheme p-n junction Na0.6CoO2/g-C3N4 heterostructure as an efficient photocatalyst for green hydrogen production: Fabrication, characterization and mechanisms. *Chem. Eng. J.* **2024**, *490*, 151408. https://doi.org/10.1016/j.cej.2024.151408.
54. Gao, Z.; Zhang, Q.; Bai, Y.; et al. Constructing Ru single atoms decorated Cu_2O for efficient CoFe-LDH/$BiVO_4$ photoanode photoelectrochemical nitrogen reduction. *J. Environ. Chem. Eng.* **2025**, *13*, 117425. https://doi.org/10.1016/j.jece.2025.117425.
55. Huang, H.; Periyanagounder, D.; Chen, C.; et al. Artificial Leaf for Solar-Driven Ammonia Conversion at Milligram-Scale Using Triple Junction III-V Photoelectrode. *Adv Sci (Weinh)* **2023**, *10*, e2205808. https://doi.org/10.1002/advs.202205808.
56. Arunachalam, M.; Ahn, K.S.; Zhu, K.; et al. Advancing Photo (Electro) Chemical Water Splitting: The Promise of Atomically Dispersed Single-, Dual-, and Alloy-Site Catalysts. *Adv. Mater. Technol.* **2025**, *11*, e00926.
57. Feng, C.; Raziq, F.; Huang, H.; et al. Shining Light on Hydrogen: Solar-Powered Catalysis with Transition Metals. *Adv. Mater.* **2025**, *37*, 2410387.
58. Wang, H.; Bai, Y.; Wang, R.; et al. Boosting photoelectrochemical water splitting: Enhanced hole transport in BiVO 4 photoanodes via interfacial coupling. *Catal. Sci. Technol.* **2025**, *15*, 405–415.
59. Wong, M.K.; Loh, J.Y.; Yap, F.M.; et al. Fueling the future of clean energy with self-supported layered double hydroxides-based electrocatalysts: A step toward sustainability. *InfoMat* **2025**, *7*, e12639.
60. Arivuthilagam, I.S.; Shahid, R.; Rahman, M.M.; et al. Advancements in Single-Atom Catalysts: Synthesis, Characterization, and Applications in Sensing Technologies. *Small Sci.* **2025**, *5*, e202500449.
61. Melchionna, M.; Fornasiero, P. On the Tracks to "Smart" Single-Atom Catalysts. *J. Am. Chem. Soc.* **2025**, *147*, 2275–2290.
62. Jiang, L.; Bai, X.; Zhi, X.; et al. New mechanistic insights into electrokinetic competition between nitrogen reduction and hydrogen evolution reactions. *Adv. Energy Mater.* **2024**, *14*, 2303809.
63. Zhang, S.; Song, Y.; Liu, Y.; et al. Conjugated Coordination Polymers with Well-Defined Single-Atom Metal Sites for Efficient Nitrogen Electroreduction to Ammonia. *Adv. Funct. Mater.* **2026**, *36*, e02874. https://doi.org/10.1002/adfm.202502874.
64. Zhang, Q.; Guan, J. Single-Atom Catalysts for Electrocatalytic Applications. *Adv. Funct. Mater.* **2020**, *30*, 2000768. https://doi.org/10.1002/adfm.202000768.
65. Peramaiah, K.; Ramalingam, V.; Fu, H.-C.; et al. Optically and Electrocatalytically Decoupled Si Photocathodes with a Porous Carbon Nitride Catalyst for Nitrogen Reduction with Over 61.8% Faradaic Efficiency. *Adv. Mater.* **2021**, *33*, 2100812. https://doi.org/10.1002/adma.202100812.
66. Gnanasekar, P.; Peramaiah, K.; Zhang, H.; et al. Protecting and Enhancing the Photoelectrocatalytic Performance of InGaN Nanowires toward Nitrogen Reduction to Ammonia Synthesis. *ACS Appl. Energy Mater.* **2023**, *6*, 10784–10793. https://doi.org/10.1021/acsaem.3c01277.
67. Chen, K.; Xu, X.; Mei, Q.; et al. Porous $TiWO_3$/$SrWO_4$ with high titanium molar ratio for efficient photoelectrocatalytic nitrogen reduction under mild conditions. *Appl. Catal. B: Environ.* **2024**, *341*, 123299. https://doi.org/10.1016/j.apcatb.2023.123299.
68. Wen, W.; Fang, S.; Zhou, Y.; et al. Modulating the Electrolyte Microenvironment in Electrical Double Layer for Boosting Electrocatalytic Nitrate Reduction to Ammonia. *Angew. Chem. Int. Ed.* **2024**, *63*, e202408382. https://doi.org/10.1002/anie.202408382.
69. Thapa, L.; Retna Raj, C. Nitrogen Electrocatalysis: Electrolyte Engineering Strategies to Boost Faradaic Efficiency. *ChemSusChem* **2023**, *16*, e202300465. https://doi.org/10.1002/cssc.202300465.
70. Huang, H.; Tu, W.; Fang, L.; et al. Lithium-Mediated Photoelectrochemical Ammonia Synthesis with 95% Selectivity on Silicon Photocathode. *ACS Energy Lett.* **2023**, *8*, 4235–4241. https://doi.org/10.1021/acsenergylett.3c01555.
71. Karamad, M.; Goncalves, T.J.; Jimenez-Villegas, S.; et al. Why copper catalyzes electrochemical reduction of nitrate to ammonia. *Faraday Discuss.* **2023**, *243*, 502–519. https://doi.org/10.1039/d2fd00145d.
72. Wu, Z.; Song, Y.; Liu, Y.; et al. Electrocatalytic nitrate reduction: Selectivity at the crossroads between ammonia and nitrogen. *Chem. Catal.* **2023**, *3*, 100786. https://doi.org/10.1016/j.checat.2023.100786.
73. Ge, X.; Jing, Y.; An, N.; et al. Layered Double Hydroxides as Building Blocks for Precise Catalysis. *Angew. Chem. Int. Ed.* **2025**, *64*, e202517103. https://doi.org/10.1002/anie.202517103.
74. Taoufik, N.; Sadiq, M.h.; Abdennouri, M.; et al. Recent advances in the synthesis and environmental catalytic applications of layered double hydroxides-based materials for degradation of emerging pollutants through advanced oxidation processes. *Mater. Res. Bull.* **2022**, *154*, 111924. https://doi.org/10.1016/j.materresbull.2022.111924.
75. Jin, W.; Go, H.; Jeong, J.; et al. Nickel Hydroxide Catalyzed Bias-free Photoelectrochemical NH3 Production via Nitrate Reduction. *Adv. Mater.* **2025**, *37*, 2506567. https://doi.org/10.1002/adma.202506567.
76. Bai, Y.; Fang, Z.; Lei, Y.; et al. FCF-LDH/BiVO4 with synergistic effect of physical enrichment and chemical adsorption for efficient reduction of nitrate. *Green. Energy Environ.* **2024**, *9*, 1112–1121. https://doi.org/10.1016/j.gee.2023.05.011.
77. Strmcnik, D.; Genorio, B.; Danilovic, N.; et al. Interfacial Electrochemistry of Chemically Modified Electrode Materials, Relevant for Energy Conversion and Storage Systems. *ECS Meet. Abstr.* **2018**, *37*, 2168–2168. https://doi.org/10.1149/ma2018-01/37/2168.

78. Zhang, M.; Li, X.; Zhao, J.; et al. Surface/interface engineering of noble-metals and transition metal-based compounds for electrocatalytic applications. *J. Mater. Sci. Amp; Technol.* **2020**, *38*, 221–236. https://doi.org/10.1016/j.jmst.2019.07.040.
79. Ren, S.; Gao, R.T.; Nguyen, N.T.; et al. Enhanced Charge Carrier Dynamics on Sb(2) Se(3) Photocathodes for Efficient Photoelectrochemical Nitrate Reduction to Ammonia. *Angew. Chem. Int. Ed. Engl.* **2024**, *63*, e202317414. https://doi.org/10.1002/anie.202317414.
80. Kim, H.E.; Kim, J.; Ra, E.C.; et al. Photoelectrochemical Nitrate Reduction to Ammonia on Ordered Silicon Nanowire Array Photocathodes. *Angew. Chem. Int. Ed. Engl.* **2022**, *61*, e202204117. https://doi.org/10.1002/anie.202204117.
81. Song, K.; Liu, H.; Chen, B.; et al. Toward efficient utilization of photogenerated charge carriers in photoelectrochemical systems: Engineering strategies from the atomic level to configuration. *Chem. Rev.* **2024**, *124*, 13660–13680.
82. Chen, L.; Ren, J.T.; Yuan, Z.Y. Enabling internal electric fields to enhance energy and environmental catalysis. *Adv. Energy Mater.* **2023**, *13*, 2203720.
83. Sun, F.; Zhang, W.; Yu, F.; et al. Heterojunction Catalysts for Enhanced Electrochemical Nitrate Reduction to Ammonia: Mechanisms, Advances, and Prospects. *Small* **2025**, *21*, e09169. https://doi.org/10.1002/smll.202509169.
84. Ma, W.; Du, S.; Suo, S.; et al. Piezoelectric field accelerating charge transfer in Z-scheme heterojunction 2D-KNbO3/1D-CdS for efficient piezo-photocatalytic H2 evolution and TCH degradation. *Surf. Interfaces* **2024**, *54*, 105240. https://doi.org/10.1016/j.surfin.2024.105240.
85. Kim, Y.; Kim, J.H.; Lee, E.; et al. Bias-Free Solar Upcycling of Nitrate and Glycerol with Highly Efficient and Durable Organic Semiconductor-Based Photoelectrodes. *Adv. Mater.* **2025**, *37*, e07698. https://doi.org/10.1002/adma.202507698.
86. Ding, J.; Lyu, Y.; Zhou, H.; et al. Efficiently unbiased solar-to-ammonia conversion by photoelectrochemical Cu/C/Si-TiO2 tandems. *Appl. Catal. B: Environ. Energy* **2024**, *345*, 123735. https://doi.org/10.1016/j.apcatb.2024.123735.
87. Han, C.; Li, C.; Yuwono, J.A.; et al. Nanostructured hybrid catalysts empower the artificial leaf for solar-driven ammonia production from nitrate. *Energy Environ. Sci.* **2024**, *17*, 5653–5665. https://doi.org/10.1039/d3ee03836j.
88. Bai, H.; Wang, F.; Ding, Q.; et al. Construction of Frustrated Lewis Pair Sites in CeO(2)-C/BiVO(4) for Photoelectrochemical Nitrate Reduction. *Inorg. Chem.* **2023**, *62*, 2394–2403. https://doi.org/10.1021/acs.inorgchem.2c04208.
89. Tripathy, S.R.; Baral, S.S. Defect Engineering in Semiconductor Photocatalysts: Enhancing Photocatalytic Activity for Green Energy Production. *Adv. Energy Sustain. Res.* **2025**, *6*, 2500110. https://doi.org/10.1002/aesr.202500110.
90. Tu, S.; Li, J.; Wu, T.; et al. Recent Advances in the Application of Transition Metal-Based Catalysts in Electrocatalytic Ammonia Synthesis and CN Bond Formation. *J. Mater. Chem. A* **2026**, *14*, 1383–1421.
91. Tu, W.; Xu, Y.; Wang, J.; et al. Investigating the Role of Tunable Nitrogen Vacancies in Graphitic Carbon Nitride Nanosheets for Efficient Visible-Light-Driven H₂ Evolution and CO₂ Reduction. *ACS Sustain. Chem. Amp; Eng.* **2017**, *5*, 7260–7268. https://doi.org/10.1021/acssuschemeng.7b01477.
92. Li, M.; Shi, Q.; Li, Z.; et al. Photoelectrocatalytic Synthesis of Urea from Carbon Dioxide and Nitrate over a Cu(2)O Photocathode. *Angew. Chem. Int. Ed. Engl.* **2024**, *63*, e202406515. https://doi.org/10.1002/anie.202406515.
93. Zhou, S.; Sun, K.; Toe, C.Y.; et al. Engineering a Kesterite-Based Photocathode for Photoelectrochemical Ammonia Synthesis from NO(x) Reduction. *Adv. Mater.* **2022**, *34*, e2201670. https://doi.org/10.1002/adma.202201670.
94. Xu, S.; Ruan, X.; Ganesan, M.; et al. Transition metal-based catalysts for urea oxidation reaction (UOR): Catalyst design strategies, applications, and future perspectives. *Adv. Funct. Mater.* **2024**, *34*, 2313309.
95. Fu, X.; Wan, C.; Huang, Y.; et al. Noble metal based electrocatalysts for alcohol oxidation reactions in alkaline media. *Adv. Funct. Mater.* **2022**, *32*, 2106401.
96. Goetz, M.K.; Bender, M.T.; Choi, K.-S. Predictive control of selective secondary alcohol oxidation of glycerol on NiOOH. *Nat. Commun.* **2022**, *13*, 5848.
97. Li, J.; Ma, Y.; Mu, X.; et al. Recent Advances and Perspectives on Coupled Water Electrolysis for Energy-Saving Hydrogen Production. *Adv. Sci.* **2025**, *12*, 2411964.
98. Liu, T.K.; Jang, G.Y.; Kim, S.; et al. Organic upgrading through photoelectrochemical reactions: Toward higher profits. *Small Methods* **2024**, *8*, 2300315.
99. Chu, S.; Zhang, B.; Zhao, X.; et al. Photocatalytic Conversion of Plastic Waste: From Photodegradation to Photosynthesis. *Adv. Energy Mater.* **2022**, *12*, 2200435. https://doi.org/10.1002/aenm.202200435.
100. Tang, D.; Lu, G.; Shen, Z.; et al. A review on photo-, electro- and photoelectro- catalytic strategies for selective oxidation of alcohols. *J. Energy Chem.* **2023**, *77*, 80–118. https://doi.org/10.1016/j.jechem.2022.10.038.
101. Hill, C.K.; Hartwig, J.F. Site-selective oxidation, amination and epimerization reactions of complex polyols enabled by transfer hydrogenation. *Nat. Chem.* **2017**, *9*, 1213–1221. https://doi.org/10.1038/nchem.2835.
102. Suri, D.; Das, S.; Choudhary, S.; et al. Enigma of sustainable CO2 conversion to renewable fuels and chemicals through photocatalysis, electrocatalysis, and photoelectrocatalysis: Design strategies and atomic level insights. *Small* **2025**, *21*, 2408981.
103. Xiong, P.; Xu, H.-C. Molecular Photoelectrocatalysis for Radical Reactions. *Acc. Chem. Res.* **2025**, *58*, 299–311. https://doi.org/10.1021/acs.accounts.4c00739.

104. Li, P.; Zhang, T.; Mushtaq, M.A.; et al. Research Progress in Organic Synthesis by Means of Photoelectrocatalysis. *Chem. Rec.* **2021**, *21*, 841–857. https://doi.org/10.1002/tcr.202000186.
105. Tang, X.; Xin, Y.; Chen, R.; et al. Advancements in water electrolysis: Enhancing hydrogen and oxygen production efficiency through electrocatalyst design and urea oxidation. *J. Mater. Chem. A* **2025**, *13*, 34122–34148.
106. Andersson, A.; Holmberg, J.; Häggblad, R. Process Improvements in Methanol Oxidation to Formaldehyde: Application and Catalyst Development. *Top. Catal.* **2016**, *59*, 1589–1599. https://doi.org/10.1007/s11244-016-0680-1.
107. Lin, Y.; Chen, Y.; Ren, H.; et al. Inspiration of Bimetallic Peroxide for Controllable Electrooxidizing Ethylene Glycol Through Modulating Surficial Intermediates. *Adv. Funct. Mater.* **2024**, *34*, 2404594. https://doi.org/10.1002/adfm.202404594.
108. Zhao, J.-J.; Zhu, H.-R.; Huang, C.-J.; et al. Recent advances of ethylene glycol oxidation reaction: Catalytic mechanism, catalyst design and applications. *J. Mater. Chem. A* **2025**, *13*, 3236–3272. https://doi.org/10.1039/d4ta07455f.
109. Kuo, H.-H.; Vo, T.-G.; Hsu, Y.-J. From sunlight to valuable molecules: A journey through photocatalytic and photoelectrochemical glycerol oxidation towards valuable chemical products. *J. Photochem. Photobiol. C: Photochem. Rev.* **2024**, *58*, 100649. https://doi.org/10.1016/j.jphotochemrev.2023.100649.
110. Vilanova, A.; Dias, P.; Lopes, T.; et al. The route for commercial photoelectrochemical water splitting: A review of large-area devices and key upscaling challenges. *Chem. Soc. Rev.* **2024**, *53*, 2388–2434.
111. Ma, G.; Jiang, N.; Song, D.; et al. Efficient strategies for designing photoanodes toward selective photoelectrochemical glycerol upgrading: A review. *J. Mater. Chem. A* **2025**, *13*, 889–917.
112. Jin, C.; Han, M.; Wu, Y.; et al. Solar-driven photoelectrochemical conversion of biomass: Recent progress, mechanistic insights and potential scalability. *Energy Environ. Sci.* **2024**, *17*, 7459–7511.
113. Gao, X.; Zhang, S.; Wang, P.; et al. Urea catalytic oxidation for energy and environmental applications. *Chem. Soc. Rev.* **2024**, *53*, 1552–1591. https://doi.org/10.1039/d3cs00963g.
114. Wang, P.; Li, J.; Xu, Y.; et al. Efficient Hydrogen Generation and Total Nitrogen Removal for Urine Treatment in a Neutral Solution Based on a Self-Driving Nano Photoelectrocatalytic System. *Nanomaterials* **2021**, *11*, 2777. https://doi.org/10.3390/nano11112777.
115. Shaheen, A.; Anwar, N.; Chen, F.; et al. Materials Interface Engineering: Impact of Interfacial Molecular Orientation on Organic Electronic Devices. *Adv. Funct. Mater.* **2025**, *35*, 2505173.
116. Xiao, Z.; Xiao, J.; Sun, Q.; et al. Interface Engineering of Conjugated Polymer-Based Composites for Photocatalysis. *Chem. –A Eur. J.* **2022**, *28*, e202202593.
117. Rose, M.J. Semiconductor band structure, symmetry, and molecular interface hybridization for the chemist. *J. Am. Chem. Soc.* **2024**, *146*, 5735–5748.
118. Bezboruah, J.; Sanke, D.M.; Munde, A.V.; et al. Nickel-doped TiO2 and thiophene-naphthalenediimide copolymer based inorganic/organic nano-heterostructure for the enhanced photoelectrochemical urea oxidation reaction. *Int. J. Hydrog. Energy* **2023**, *48*, 7361–7373. https://doi.org/10.1016/j.ijhydene.2022.11.098.
119. Liu, J.; Li, J.; Shao, M.; et al. Directed synthesis of SnO2@BiVO4/Co-Pi photoanode for highly efficient photoelectrochemical water splitting and urea oxidation. *J. Mater. Chem. A* **2019**, *7*, 6327–6336. https://doi.org/10.1039/C8TA11573G.
120. Dang, K.; Wu, L.; Liu, S.; et al. Harnessing Adsorbate-Adsorbate Interaction to Activate C-N Bond for Exceptional Photoelectrochemical Urea Oxidation. *Angew. Chem. Int. Ed. Engl.* **2025**, *64*, e202423457. https://doi.org/10.1002/anie.202423457.
121. Gu, Y.; Zhang, X.; Zhou, L.; et al. Synergistic Integration of nickel sulfide clusters in hierarchical perylene-polyimide conductive frameworks for energy-efficient electrochemical urea oxidation reaction. *J. Alloys Compd.* **2025**, *1041*, 183753. https://doi.org/10.1016/j.jallcom.2025.183753.
122. Ge, J.; Kuang, J.; Xiao, Y.; et al. Recent development of nickel-based catalysts and in situ characterization techniques for mechanism understanding of the urea oxidation reaction. *Surf. Interfaces* **2023**, *41*, 103230. https://doi.org/10.1016/j.surfin.2023.103230.
123. Zhou, C.; Li, J.; Wang, J.; et al. Efficient H2 production and TN removal for urine disposal using a novel photoelectrocatalytic system of Co_3O_4/$BiVO_4$-MoNiCuO_x/Cu. *Appl. Catal. B: Environ.* **2023**, *324*, 122229. https://doi.org/10.1016/j.apcatb.2022.122229.
124. Lyu, Z.-H.; Fu, J.; Tang, T.; et al. Design of ammonia oxidation electrocatalysts for efficient direct ammonia fuel cells. *EnergyChem* **2023**, *5*, 100093. https://doi.org/10.1016/j.enchem.2022.100093.
125. Zhou, J.; Guan, B.; Guo, J.; et al. Review of the catalytic system, synthetic process, and support morphological research in selective catalytic oxidation of ammonia. *Ind. Eng. Chem. Res.* **2023**, *62*, 20506–20546.
126. Han, C.; Wang, K. Recent Advances in Photoelectrochemical Synthesis of Nitrogen-Containing Solar Fuels and Chemicals. *Energy Fuels* **2025**, *39*, 16065–16077.
127. Cechanaviciute, I.A.; Schuhmann, W. Electrocatalytic Ammonia Oxidation Reaction: Selective Formation of Nitrite and Nitrate as Value-Added Products. *ChemSusChem* **2025**, *18*, e202402516.

128. Huang, Q.-X.; Wang, F.; Liu, Y.; et al. Recent progress of two-dimensional metal-base catalysts in urea oxidation reaction. *Rare Met.* **2024**, *43*, 3607–3633. https://doi.org/10.1007/s12598-024-02668-y.
129. Xia, C.; Li, Y.; Kim, H.; et al. A highly activated iron phosphate over-layer for enhancing photoelectrochemical ammonia decomposition. *J. Hazard. Mater.* **2021**, *408*, 124900. https://doi.org/10.1016/j.jhazmat.2020.124900.
130. Wu, L.; Tang, D.; Xue, J.; et al. Competitive Non-Radical Nucleophilic Attack Pathways for NH3 Oxidation and H2O Oxidation on Hematite Photoanodes. *Angew. Chem. Int. Ed.* **2022**, *61*, e202214580. https://doi.org/10.1002/anie.202214580.
131. Wu, L.; Li, Q.; Dang, K.; et al. Highly Selective Ammonia Oxidation on BiVO4 Photoanodes Co-catalyzed by Trace Amounts of Copper Ions. *Angew. Chem.* **2024**, *136*, e202316218.
132. Shi, Q.; Duan, H. Recent progress in photoelectrocatalysis beyond water oxidation. *Chem. Catal.* **2022**, *2*, 3471–3496.
133. Sun, D.; Zhang, Y.; Zhou, Y.; et al. Photocatalytic and electrochemical synthesis of biofuel via efficient valorization of biomass. *Adv. Energy Mater.* **2025**, *15*, 2406098.
134. Luo, H.; Barrio, J.; Sunny, N.; et al. Progress and perspectives in photo-and electrochemical-oxidation of biomass for sustainable chemicals and hydrogen production. *Adv. Energy Mater.* **2021**, *11*, 2101180.
135. Qiu, J.; Forbes, T.; Lin, T. Tailoring the oxidation of benzyl alcohol and its derivatives with (photo) electrocatalysis. *Chem. Commun.* **2025**, *61*, 3421–3435.
136. Zhu, P.; Shen, Y.; Zhang, Z.-M.; et al. Modulating alcohol adsorption modes for boosting electrooxidation-assisted hydrogen production. *ACS Catal.* **2024**, *14*, 7674–7683.
137. Gao, L.; Cui, X.; Sewell, C.D.; et al. Recent advances in activating surface reconstruction for the high-efficiency oxygen evolution reaction. *Chem. Soc. Rev.* **2021**, *50*, 8428–8469.
138. Zhang, W.; Huang, B.; Cui, Y.; et al. Investigation of the mechanism of methanol electrooxidation: A potential-dependent DFT study. *RSC Adv.* **2025**, *15*, 11056–11064. https://doi.org/10.1039/d5ra01511a.
139. Zhou, H.; Zhang, D.; Xie, H.; et al. Modulating Oxygen Vacancies in Lead Chromate for Photoelectrocatalytic Water Splitting. *Adv. Mater.* **2023**, *35*, 2300914. https://doi.org/10.1002/adma.202300914.
140. Xie, S.; Shen, Z.; Deng, J.; et al. Visible light-driven C−H activation and C–C coupling of methanol into ethylene glycol. *Nat. Commun.* **2018**, *9*, 1181.
141. Yao, S.; Ou Yang, F.; Shimumora, S.; et al. A kinetic study of methanol oxidation over SiO2. *Appl. Catal. A: Gen.* **2000**, *198*, 43–50. https://doi.org/10.1016/s0926-860x(99)00505-0.
142. Li, S.; Chen, F.; Ma, T.; et al. Vacancy engineered BiVO4 photoanode realizes efficient photoelectrochemical CH3OH oxidation in near-neutral media: Active site regulation improves HCHO selectivity. *Chem. Eng. J.* **2023**, *467*, 143421. https://doi.org/10.1016/j.cej.2023.143421.
143. Lima, P.J.M.; da Silva, R.M.; Neto, C.A.C.G.; et al. An overview on the conversion of glycerol to value-added industrial products via chemical and biochemical routes. *Biotechnol. Appl. Biochem.* **2022**, *69*, 2794–2818.
144. Li, Z.; Luo, L.; Li, M.; et al. Photoelectrocatalytic C–H halogenation over an oxygen vacancy-rich TiO2 photoanode. *Nat. Commun.* **2021**, *12*, 6698. https://doi.org/10.1038/s41467-021-26997-z.
145. Lu, Y.; Lee, B.G.; Lin, C.; et al. Solar-driven highly selective conversion of glycerol to dihydroxyacetone using surface atom engineered BiVO4 photoanodes. *Nat. Commun.* **2024**, *15*, 5475. https://doi.org/10.1038/s41467-024-49662-7.
146. Tian, Z.; Da, Y.; Wang, M.; et al. Selective photoelectrochemical oxidation of glucose to glucaric acid by single atom Pt decorated defective TiO_2. *Nat. Commun.* **2023**, *14*, 142. https://doi.org/10.1038/s41467-023-35875-9.
147. Ding, C.; Shi, J.; Wang, Z.; et al. Photoelectrocatalytic Water Splitting: Significance of Cocatalysts, Electrolyte, and Interfaces. *ACS Catal.* **2017**, *7*, 675–688. https://doi.org/10.1021/acscatal.6b03107.
148. Yang, J.; Wang, D.; Han, H.; et al. Roles of Cocatalysts in Photocatalysis and Photoelectrocatalysis. *Acc. Chem. Res.* **2013**, *46*, 1900–1909. https://doi.org/10.1021/ar300227e.
149. Sultana, S.; Darowska, I.; Pisarek, M.; et al. Designing TiO2 Nanotubular Arrays with Au-CoOx Core–Shell Nanoparticles for Enhanced Photoelectrochemical Methanol and Lignin Oxidation. *ACS Appl. Mater. Interfaces* **2024**, *16*, 49262–49274. https://doi.org/10.1021/acsami.4c07498.
150. Zheng, B.-F.; Ouyang, T.; Wang, Z.; et al. Enhanced plasmon-driven photoelectrocatalytic methanol oxidation on Au decorated α-Fe2O3 nanotube arrays. *Chem. Commun.* **2018**, *54*, 9583–9586. https://doi.org/10.1039/c8cc04199g.
151. Wang, L.; Mitoraj, D.; Turner, S.; et al. Ultrasmall CoO(OH)x Nanoparticles As a Highly Efficient "True" Cocatalyst in Porous Photoanodes for Water Splitting. *ACS Catal.* **2017**, *7*, 4759–4767. https://doi.org/10.1021/acscatal.7b01466.
152. Kang, F.; Wang, Q.; Du, D.; et al. Photoelectrochemical Ethylene Glycol Oxidization Coupled with Hydrogen Generation Using Metal Oxide Photoelectrodes. *Angew. Chem. Int. Ed.* **2025**, *137*, e202417648. https://doi.org/10.1002/anie.202417648.
153. Manna, S.; Satpati, A.K.; Patra, C.N.; et al. Enhancing the PEC Efficiency in the Perspective of Crystal Facet Engineering and Modulation of Surfaces. *ACS Omega* **2024**, *9*, 6128–6146. https://doi.org/10.1021/acsomega.3c07867.
154. Liu, D.; Liu, J.-C.; Cai, W.; et al. Selective photoelectrochemical oxidation of glycerol to high value-added dihydroxyacetone. *Nat. Commun.* **2019**, *10*, 1779. https://doi.org/10.1038/s41467-019-09788-5.

155. Vo, T.-G.; Kao, C.-C.; Kuo, J.-L.; et al. Unveiling the crystallographic facet dependence of the photoelectrochemical glycerol oxidation on bismuth vanadate. *Appl. Catal. B: Environ.* **2020**, *278*, 119303. https://doi.org/10.1016/j.apcatb.2020.119303.
156. Wang, Z.; Gao, Y.; Lu, Y.; et al. BiV1–xOy/Noble Metal Nanoparticle Domains with Reverse Charge Transfer Improves Photoelectrochemical Glycerol to Dihydroxyacetone Conversion. *J. Am. Chem. Soc.* **2025**, *147*, 40136–40145. https://doi.org/10.1021/jacs.5c06621.
157. An, Y.; Yang, X.; Wang, R.; et al. Improving Tandem Epoxidation Efficiency via Hydrogel Confinement Effect towards Photoelectrochemical Propylene Oxide Synthesis. *Angew. Chem. Int. Ed.* **2025**, *64*, e202518020. https://doi.org/10.1002/anie.202518020.
158. Zhao, Y.; Adiyeri Saseendran, D.P.; Huang, C.; et al. Oxygen Evolution/Reduction Reaction Catalysts: From In Situ Monitoring and Reaction Mechanisms to Rational Design. *Chem. Rev.* **2023**, *123*, 6257–6358. https://doi.org/10.1021/acs.chemrev.2c00515.
159. Wu, X.; Zhao, Z.-J.; Shi, X.; et al. Multi-site catalysis of high-entropy hydroxides for sustainable electrooxidation of glucose to glucaric acid. *Energy Environ. Sci.* **2024**, *17*, 3042–3051. https://doi.org/10.1039/D4EE00221K.
160. Yang, C.; Li, Z.; Xu, J.; et al. Electrocatalytic C–N coupling for urea synthesis: A critical review. *Green. Chem.* **2024**, *26*, 4908–4933. https://doi.org/10.1039/d3gc04920e.
161. Yang, Y.; Guo, S.; Miao, J.; et al. Bias-Free Photoelectrochemical Nitrobenzene-to-Aniline Conversion via a Bidirectional Hydrogen Balance System. *ACS Catal.* **2025**, *15*, 17581–17590. https://doi.org/10.1021/acscatal.5c05682.
162. Zhang, Q.; Chen, C.; Qu, G.; et al. Different methanol oxidation behaviors on defectively nanoporous hematite photoanode modified with platinum via photoreduction versus electrodeposition. *J. Alloys Compd.* **2024**, *976*, 173244. https://doi.org/10.1016/j.jallcom.2023.173244.
163. Huang, S.; Feng, F.; Huang, R.T.; et al. Activating C–H Bonds by Tuning Fe Sites and an Interfacial Effect for Enhanced Methanol Oxidation. *Adv. Mater.* **2022**, *34*, 2208438. https://doi.org/10.1002/adma.202208438.
164. Wadhwa, R.; Yadav, K.K.; Goswami, T.; et al. Mechanistic Insights for Photoelectrochemical Ethanol Oxidation on Black Gold Decorated Monoclinic Zirconia. *ACS Appl. Mater. Interfaces* **2021**, *13*, 9942–9954. https://doi.org/10.1021/acsami.0c21010.
165. Huang, S.; Ouyang, T.; Zheng, B.F.; et al. Enhanced Photoelectrocatalytic Activities for CH_3OH-to-HCHO Conversion on Fe_2O_3/MoO_3: Fe-O-Mo Covalency Dominates the Intrinsic Activity. *Angew. Chem. Int. Ed.* **2021**, *60*, 9546–9552. https://doi.org/10.1002/anie.202101058.
166. Zhang, K.; Wang, C.; Guo, S.; et al. Photoelectrocatalytic oxidation of ethylene glycol on trimetallic PdAgCu nanospheres enhanced by surface plasmon resonance. *J. Colloid. Interface Sci.* **2023**, *636*, 559–567. https://doi.org/10.1016/j.jcis.2023.01.055.
167. Xu, H.; Song, P.; Yan, B.; et al. Surface-Plasmon-Enhanced Photo-electrocatalytic Ethylene Glycol Oxidation Based on Highly Open AuAg Nanobowls. *ACS Sustain. Chem. Eng.* **2018**, *6*, 4138–4146. https://doi.org/10.1021/acssuschemeng.7b04560.
168. Gu, Z.; An, X.; Liu, R.; et al. Interface-modulated nanojunction and microfluidic platform for photoelectrocatalytic chemicals upgrading. *Appl. Catal. B: Environ.* **2021**, *282*, 119541. https://doi.org/10.1016/j.apcatb.2020.119541.
169. Xiao, Y.; Wang, M.; Liu, D.; et al. Selective Photoelectrochemical Oxidation of Glycerol to Glyceric Acid on (002) Facets Exposed WO_3 Nanosheets. *Angew. Chem. Int. Ed.* **2024**, *63*, e202319685. https://doi.org/10.1002/anie.202319685.
170. Zhou, Z.; Xie, Y.-N.; Zhu, W.; et al. Selective photoelectrocatalytic tuning of benzyl alcohol to benzaldehyde for enhanced hydrogen production. *Appl. Catal. B Environ.* **2021**, *286*, 119868. https://doi.org/10.1016/j.apcatb.2020.119868.
171. Sun, J.; Wang, B.; Nie, Z.; et al. Selective Oxidation of Alcohol to Valuable Aldehydes Using Water as a Promoter in a Photoelectrochemical Cell. *Langmuir* **2024**, *40*, 13265–13275. https://doi.org/10.1021/acs.langmuir.4c01453.
172. Wang, Y.; Liu, D.; Qin, W.; et al. Synergistic interfacial and radical strategy enables boosted near-neutral selective photoelectrochemical alcohol oxidation. *J. Catal.* **2025**, *448*, 116161. https://doi.org/10.1016/j.jcat.2025.116161.